Department of Defense
Legacy Resource Management Program

PROJECT NUMBER 14-766

WHITE-NOSE SYNDROME EARLY DETECTION AND MONITORING FOR MILITARY TRAINING FACILITIES

TECHNICAL REPORT: BASELINE FUNGAL COMMUNITY ANALYSIS AND INVESTIGATION FOR *PSEUDOGYMNOASCUS* (=*GEOMYCES*) *DESTRUCTANS* IN RESPONSE TO WHITE-NOSE SYNDROME THREAT AT FORT HOOD, CORYELL COUNTY, TEXAS

ZARA Environmental LLC

15 JAN 2016

Abstract

White-nose syndrome (WNS) has been responsible for the deaths of millions of bats in the U.S. since its introduction in 2006. The pathogen responsible for causing WNS is the fungus *Pseudogymnoascus* (=*Geomyces*) *destructans* (*Pd*), which has been confirmed in Oklahoma and Arkansas, but has not yet been detected in Texas caves. Fort Hood is an active military training base that contains several caves with known hibernacula and maternity colonies for cave myotis bats (*Myotis velifer*) and tri-colored bats (*Perimyotis subflavus).* Researchers sampled substrates in Shell Mountain Bat Cave, Tippit Cave, Doubletree Cave, and Egypt Cave and collected swabs of walls and ceilings in Shell Mountain Bat Cave in order to determine whether *Pd* was present using two recently developed polymerase chain reaction (PCR) methods. In addition, two methods were used to develop baseline fungal community information in the four study caves using a culture-independent approach that incorporated PCR using internal transcribed spacer (ITS) primers (ITS4 and ITS5) and a culture-based approach using matrix-assisted laser desorption/ionization (MALDI) mass spectrometry or sequencing 18S rRNA amplicons produced using PCR for the identification of successfully cultured isolates. The *Pd* screening effort did not result in the detection of the pathogen in the four study caves. The fungal community analysis using both methods resulted in the identification of 24 taxa consisting of representatives of Ascomycota, Basidiomycota, and Zygomycota. The continued monitoring of these four caves will help to enhance the continued mission readiness of Fort Hood by enabling early detection of *Pd* and/or symptoms of WNS such that the base can effectively respond to the risk.

Table of Contents

Abstract i
Introduction 1
Methods 3
Study Sites 3
Shell Mountain Bat Cave 3
Tippit Cave 7
Doubletree Cave 9
Egypt Cave 11
Sample Collection Methods 14
Pd Screening Methods 16
Fungal Community Detection Methods – Molecular 17
Fungal Community Detection Methods – Culturing 18
Microclimate Data Collection Methods 18
Results 19
Pd Screening Results 19
Fungal Community Detection Results 22
Microclimate Data Results 25
Discussion 27
Literature Cited 30

List of Figures

Figure 1. Plan and profile map of Shell Mountain Bat Cave, showing sampling locations for various types of substrate collected. 5
Figure 2. Plan and profile map of Shell Mountain Bat Cave, showing swab sampling locations. .. 6
Figure 3. The lower passage of Tippit Cave contains a small underground stream. 7
Figure 4. Plan and profile map of Tippit Cave, showing sampling locations for various types of substrate collected. 8
Figure 5. Doubletree Cave contains abundant loose soil and organic matter. 9
Figure 6. Plan and profile map of Doubletree Cave, showing sampling locations for various types of substrate collected. 10
Figure 7. Guano pile near sampling location EGGU08 in Egypt Cave. 11
Figure 8. Plan map of Egypt Cave, showing sampling locations for various types of substrate collected. 12
Figure 9. Profile map of Egypt Cave, showing sampling locations for various types of substrate collected. 13
Figure 10. Labeled sampling location indicating that this sample was from Egypt Cave (EG), that the substrate collected was guano (GU) and that this was sample number 8. 15
Figure 11. Negative detection of *Pd* in a representative laboratory DGGE sample set correlating with the results from 09 June 2015 (presented in Table 1). The nucleotide reference ladder is located in the far left lane, while the *Pd* screening test samples are located in

Lanes 1 through 12. The lanes labeled “Neg” and “Pos” are the negative and positive controls, respectively. 19
Figure 12. Amplification results using ITS3/4 PCR in a representative laboratory DGGE sample set correlating with the results from 11 May 2015. The nucleotide reference ladder is located in the far left lane, while the ITS3/4 amplicon samples are located in Lanes 1 through 12. The lanes labeled “Neg” and “Pos” are the negative and positive controls, respectively. 22
Figure 13. Amplification results using ITS5/5 PCR in a representative laboratory DGGE sample set correlating with the “ITS4/ITS5 Amplicon Production” column presented in Table 2. Lane 12 is the negative control and lanes 13 and 14 are the positive controls. The nucleotide reference ladders are located between lanes 8 and 9 and in the far right lane, while the ITS4/5 amplicon samples are located in lanes 1 through 11 as follows: SMGU05, SMGU06, SMGU02, SMBT01, DTGU03, DTSL04, TPSL01, TPSL05, TPMS01, EGGU03, EGGU08, EGSL09, EGSL04, and EGSL01. 25

List of Tables

Table 1. Results of the Pd screening analysis including quality control results. 21
Table 2. Fungal taxa identified using ITS4/ITS5 PCR methodology 23
Table 3. Fungal taxa identified using culturing methodology. 24
Table 4. Datalogger microclimate recordings (lows and highs) Shell Bat Cave. Adapted from Pekins (2012). 26
Table 5. Datalogger microclimate recordings (lows and highs) Tippit Cave. Adapted from Pekins (2012). 26
Table 6. Datalogger microclimate recordings (lows and highs) Egypt Cave. Adapted from Pekins (2012). 27
Table 7. Single visit December microclimate measurements. Adapted from Pekins (2012). 27

Introduction

White-nose syndrome (WNS), a disease responsible for the mortality of millions of hibernating bats in the U.S., has been spreading rapidly since its discovery in the winter of 2006 and 2007 in Schoharie County, New York. The causal agent of WNS is a psychrophilic (cold-loving), pathogenic fungus, *Pseudogymnoascus* (=*Geomyces*) *destructans* (*Pd*), that colonizes bare skin of hibernating bats (Gargas et al. 2009; Lorch et al. 2011; Minnis et al. 2013). Visible symptoms of WNS include the presence of white fungus around the muzzle, ears, and wing membranes of affected bats, where hyphae invades the epidermis and cutaneous connective tissue and leads to severe damage including skin erosions and ulcers (Blehert et al. 2009; Reichard and Kunz 2009; Meteyer et al. 2009; Lorch et al. 2011). The cutaneous mycosis provokes physiological distress, resulting in premature arousal from hibernation, dehydration, emaciation, and ultimately death. Bats exhibiting symptoms of WNS typically have little or no fat reserves and are often emaciated (Blehert et al. 2009; Warnecke et al. 2012; Verant et al. 2014). Verant et al. (2014) proposed the first holistic disease progression model for WNS that integrated the findings of previous metabolic and pathophysiological studies (Meteyer et al. 2009; Cryan et al. 2012; Reeder et al. 2012; Warnecke et al. 2012; Cryan et al. 2013; Warnecke et al. 2013) with data collected during the authors' study on *Pd*-treated little brown myotis (*Myotis lucifugus*). The integrated disease progression model indicated that bats develop a series of cascading physiological responses shortly after *Pd* colonization including the elevated use of energy, alteration of blood chemistry, an increasing rate of arousal from torpor, dehydration, emaciation, and ultimately death if energy reserves are depleted before spring emergence (Verant et al. 2014).

Currently, seven bat species have been affected by WNS including the little brown myotis, northern long-eared bat (*Myotis septentrionalis*), eastern small-footed myotis (*Myotis leibii*), Indiana myotis (*Myotis sodalis*), gray myotis (*Myotis grisescens*), big brown bat (*Eptesicus fuscus*), and tri-colored bat (*Perimyotis subflavus*; USFWS 2015a). Fort Hood, a 214,968-acre military base located near Killeen, Texas, is within the geographic range of two of the known species with confirmed diagnostic symptoms of WNS, including the tri-colored bat and big brown bat, as well as the silver-haired bat (*Lasionycteris noctivagans*), a species that has tested positive for *Pd* but with no documented diagnostic symptoms of the disease. The cave myotis (*Myotis velifer*), a species also found at Fort Hood, was suspected to carry *Pd* in 2010 when the U.S. Geological Survey (USGS) National Wildlife Health Center (NWHC) used molecular techniques (polymerase chain reaction [PCR]) to detect the fungus in samples collected from a single cave myotis mist-netted at a cave entrance in Woodward County, Oklahoma (USGS NWHC 2010). The species was removed from the list in 2014, when the USGS NWHC used improved PCR methods to reanalyze the archived samples and determined that the bat specimen did not harbor *Pd* (USGS NWHC 2014); however, cave myotis remains at risk of infection and may function as a vector of *Pd* to other vulnerable species due to its highly colonial, cave-dwelling nature. The cave myotis, which is a former category 2 candidate species for federal protection under the Endangered Species Act (ESA; USFWS 1994), is also a species of concern listed by the Texas Parks and Wildlife Department.

Recent research supports the hypothesis that *Pd* is an exotic species from Europe that was recently introduced into North America (Warnecke et al. 2012; Lorch et al. 2013; Minnis and Lindner 2013). While *Pd* has been documented throughout much of Europe, it has not been associated with unusual or extensive bat mortality (Martínková 2010; Puechmaille et al. 2010; Wibbelt et al. 2010; Puechmaille et al. 2011). The current known range of WNS in North America as of summer 2015 (USFWS 2015b) included five Canadian provinces, 26 confirmed states, and 3 states where *Pd* has been detected but with no confirmation of infection, including Oklahoma where the fungus was confirmed in May 2015 on a tri-colored bat in eastern part of the state (Oklahoma Department of Wildlife Conservation 2015), thus marking the westernmost record in the U.S. In March and May of 2015, the Arkansas Game and Fish Commission (AGFC) confirmed WNS-infected tri-colored bats in several caves in the Ozark Mountains of northern Arkansas, as well as *Pd* in mines of the Ouachita Mountains in the west-central part of the state (AGFC 2015a; AGFC 2015b). The implications of the new geographical records of *Pd* and WNS in Oklahoma and Arkansas are consequential to management interests for bats and caves in Texas because of the potential migratory connection to hibernacula in those adjacent states.

Since the sudden emergence and rapid spread of WNS in North America, natural resource managers throughout the region have been assessing the capacity for effective management of the destructive disease, including credible strategies that have a reasonable chance for success. In 2008, an effort to formalize a coordinated approach for addressing WNS was initiated among the Department of Interior, Department of Agriculture, Department of Defense (DoD), and state wildlife management agencies. Subsequently, the U.S. Fish and Wildlife Service (USFWS) implemented an adaptive national plan in 2011 that outlines the actions necessary to coordinate efforts by federal, state, tribal, and other partner entities and to manage the comprehensive investigation and response (USFWS 2011). In addition, the national plan includes cross-border coordination with the Canadian national plan (Canadian Wildlife Health Cooperative 2015), integrates with state and regional plans, and establishes seven working groups that focus on identified elements addressed by the plan, including epidemiological and ecological research; data and technical information management; diagnostics; disease management; disease surveillance; conservation and recovery; and communications and outreach. In response to the national plan, several opportunities for meeting management goals have been established or are under consideration by resource management agencies, such as developing better methods of early detection, training personnel to conduct active field surveillance and sample collection, increasing diagnostic testing of field samples, and providing additional ecological field research aimed at providing the science-based guidance needed by agencies responsible for management. Despite the implementation of the national plan and other state and regional management and response plans throughout the current known range of the disease, the continued implementation and refinement of proactive strategies is paramount as WNS continues to spread westward.

The primary objective of this study was to provide management recommendations for at-risk species to help the DoD Natural Resources Conservation Compliance Program assess the current status of *Pd* at Fort Hood. Specifically, our approach included 1) filling in regional information

gaps regarding the presence of *Pd* and baseline characterization data on the fungal communities in bat-occupied caves; 2) developing a methodology for non-invasive detection of *Pd*; 3) testing the detection methodology by implementing substrate sampling at select Fort Hood caves; and 4) developing a baseline status report detailing the methodology and results of the assessment. The development and implementation of this study is broadly applicable across other DoD installations with bats inhabiting cave roosts, especially those harboring protected species, and will maintain mission readiness in the event of positive detection by demonstrating proactive management. This study will also advance the DoD's goals described in the national plan to assist research, surveillance, disease management, diagnostic testing, and funding for WNS programs within individual DoD districts. In addition, we hope to contribute to the understanding of this emerging disease and fill regional information gaps on fungal communities in caves.

The DoD Legacy Resource Management (Legacy) Program funded this study in an effort to better understand at-risk species inhabiting Fort Hood and other DoD installations. The Legacy Program assists the DoD land managers in protecting and enhancing resources while supporting military readiness.

Methods

Study Sites

We focused our efforts on prioritizing known maternity and/or hibernation sites for tri-colored bats and cave myotis. Specifically, we selected Shell Mountain Bat Cave (SMBC), Tippit Cave, Doubletree Cave, and Egypt Cave, which are all located at Fort Hood in Coryell County, Texas. All four of the study sites are natural solution caves that developed in the lower cretaceous Edwards Group limestone (Pekins 2012; Reddell et al. 2015). Pekins (2012) and Reddell et al. (2015) provided a complete description of the four study caves, and the following section provides summary and additional details for each cave.

Shell Mountain Bat Cave

Shell Mountain Bat Cave (Figure 1 and Figure 2), located on the western portion of Fort Hood, houses a large maternity colony of cave myotis, and annual population estimates of the species at this site range from approximately 20,000 to 25,000 during the peak summer months (June through August) to a few individuals in the winter months when the bats have migrated elsewhere. Shell Mountain Bat Cave also typically supports a small population of tri-colored bats (approximately 20 individuals).

The cave, which has two entrances with box-style cupola bat gates, supports 10 known primary roosts in various locations including the main chamber, upper balcony, and a lower level room, as well as an inaccessible area of the cave that provides an undocumented roost (Pekins 2012). Moderately large guano mounds are located under the roost areas, with the largest mounds located throughout the main chamber roost. Most guano mounds under the roost areas are

seasonally fresh, identified by the presence of loose, moist, rod-shaped excrement. Older guano mounds are that are relatively dry, compacted, and stable are located in lesser-used areas and edges of active roosts. There are areas of relatively bare soil, either compacted claystone or loose clay loam, near both entrances and in areas not heavily used by roosting bats. A thin layer of guano overlies some areas of bare soil. Other organic material is present throughout the cave, including dried herbaceous vegetation (grass), leaves, seeds, wood, scat, and bat carcasses that range from relatively recently dead (with fur and tissue) to long-dead (bones only). Refuse (rusted cans and other metal objects) is scattered about the cave. Much of the cave has unrestricted airflow and good ventilation attributed to the dual entrances, although some appendage areas like the upper balcony roost have restricted airflow and poor ventilation. Surface water from precipitation events easily reaches the main chamber roost area from both entrances. The entrances of the cave are on top of a mesa ridge and surrounded by scattered brush and trees interspersed with open areas of patchy grass and rocky soil. The entrances are located in an open area with little to no vegetative canopy.

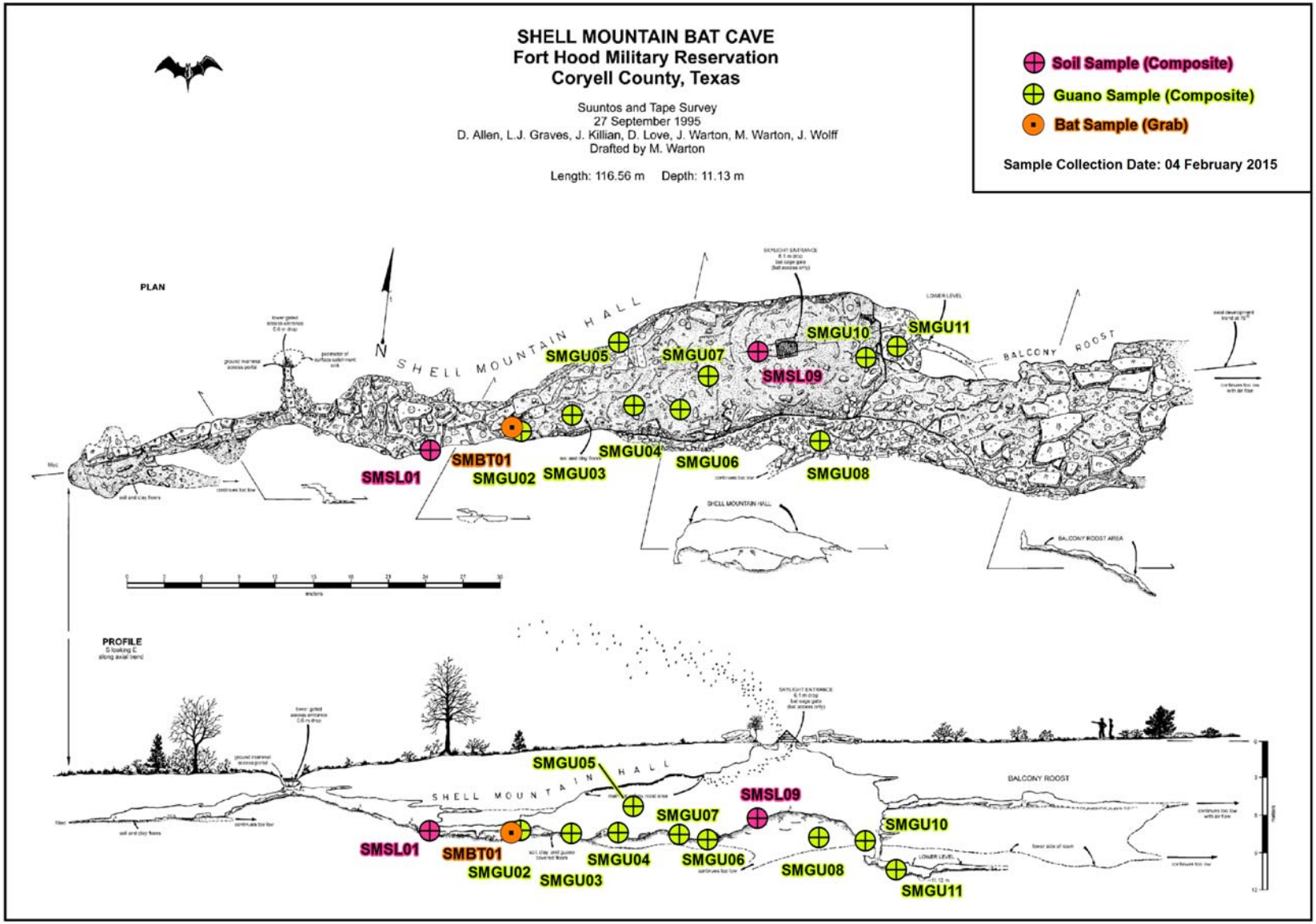

Figure 1. Plan and profile map of Shell Mountain Bat Cave, showing sampling locations for various types of substrate collected.

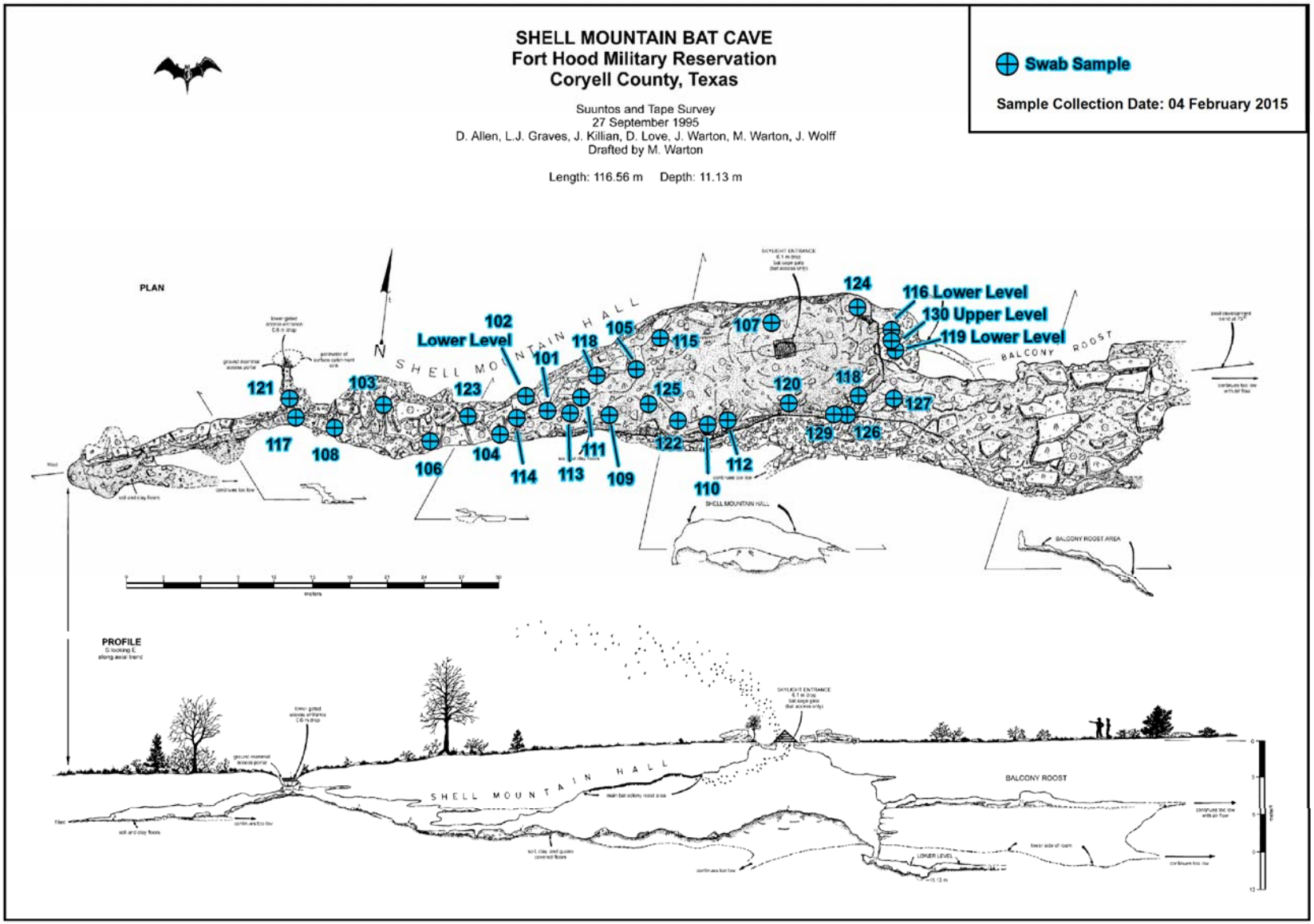

Figure 2. Plan and profile map of Shell Mountain Bat Cave, showing swab sampling locations.

Tippit Cave

Also located on top of a mesa ridge but in the eastern portion of Fort Hood, Tippit Cave (Figure 4) likely once housed a population of cave myotis (likely less than 12,000 individuals) but now typically houses approximately 10 to 20 tri-colored bats in the winter (Pekins 2012). There are six known primary roosts in the caves with moderate guano accumulation and roost stains (Pekins 2012), although most mounds in the cave appear to consist of older guano rather than relatively fresh excrement (as described further in the results). Most of the cave's visible substrate consists of compacted red claystone and limestone walls with embedded clay, and a thin layer of guano overlies many areas outside of accumulated mounds. While organic material other than guano (e.g., dried grass, leaves, scat, seeds, wood, recently dead mouse carcass) is present in some areas of the cave, most is concentrated around the sinkhole entrance and initial passage. Small tree roots are evident in some areas of the cave ceilings, even in the lower level of the cave. The cave generally has restricted airflow and relatively poor ventilation, particularly in the lower level. While surface water from precipitation events does not reach all areas of the cave (e.g., the far reaches of joint passages) from the entrance, it easily reaches the lower levels of the cave, and a small underground stream, visible through a small floor pit, flows under the floor of the lowest passage (Figure 3). The entrance of the cave is ungated and surrounded by shrubland and areas of exposed outcropping of bedrock. A wildfire in the mid-1990s burned much of the shrubland surrounding the cave entrance (Pekins 2012), although substantial regrowth of woody vegetation has occurred in the area since the fire.

Figure 3. The lower passage of Tippit Cave contains a small underground stream.

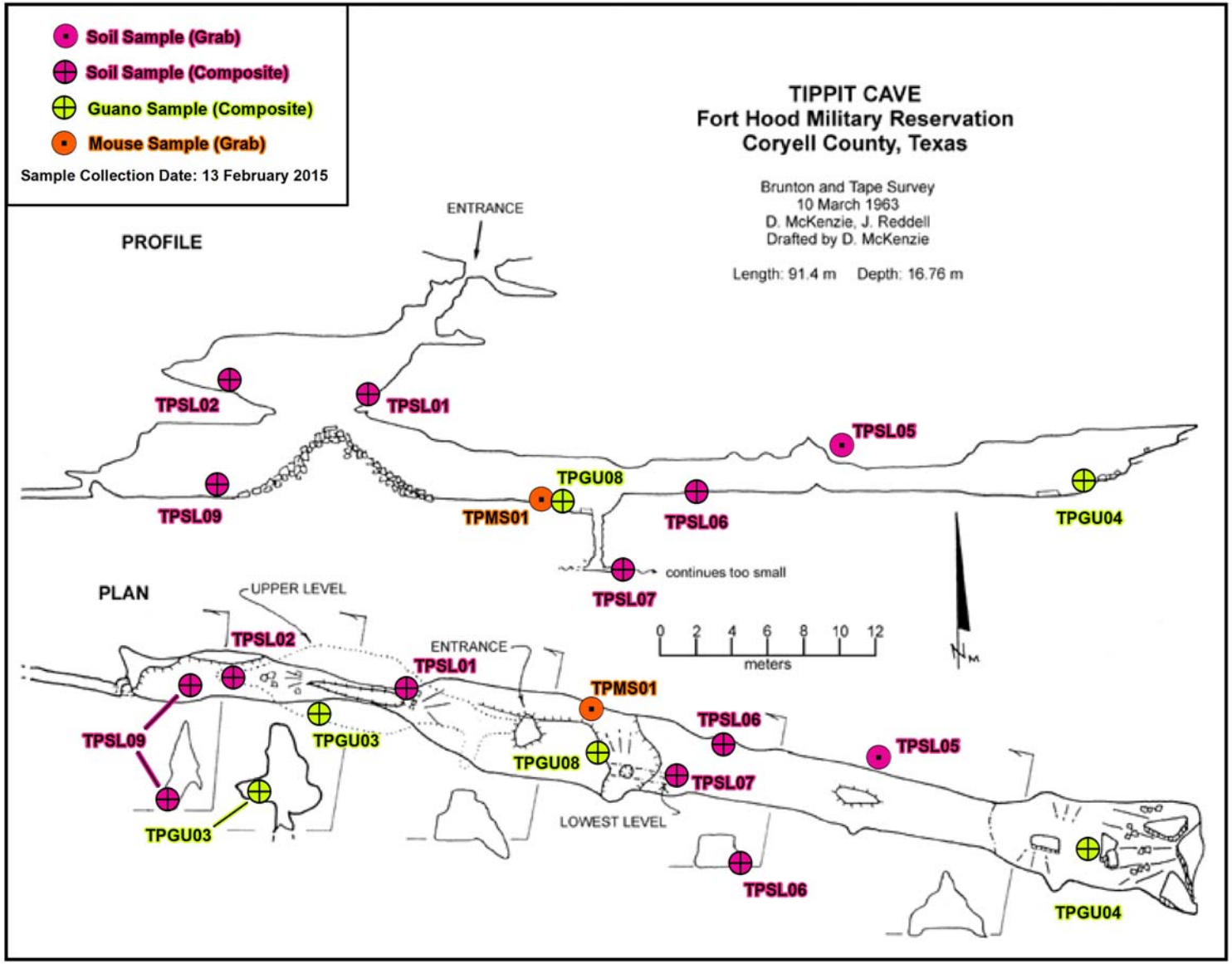

Figure 4. Plan and profile map of Tippit Cave, showing sampling locations for various types of substrate collected.

Doubletree Cave

Doubletree Cave (Figure 6) is a component of the Rocket River Cave System, one of the longest cave systems in Texas at approximately 2,572 m in length (Reddell et al. 2015). The cave, located approximately 240 m from Tippit Cave on the same shrubland-covered mesa ridge, is relatively small, harboring a few individuals (approximately 3 to 5) of tri-colored bats in the winter (Pekins 2012). The primary chamber of the cave contains roost stains and mounds that primarily consist of older guano, and a relatively high percentage of other organic matter (e.g., dried grass, leaves, wood, seeds, scat; Figure 5) is present compared to the other three caves, primarily attributed to the cave's small size. Small tree roots are evident throughout the ceiling and walls of the primary chamber. Dark, loose clay and clay loam is also present in areas not covered in guano, such as the main chamber side passage and lower level that connects to the Rocket River Cave underground stream. The cave mostly has unrestricted airflow and good ventilation attributed to its connection with the Rocket River Cave System. Surface water from precipitation events easily reaches the lower level of the cave from the entrance and eventually flows into the Rocket River Cave underground stream. The cave entrance has a box-style cupola bat gate.

Figure 5. Doubletree Cave contains abundant loose soil and organic matter.

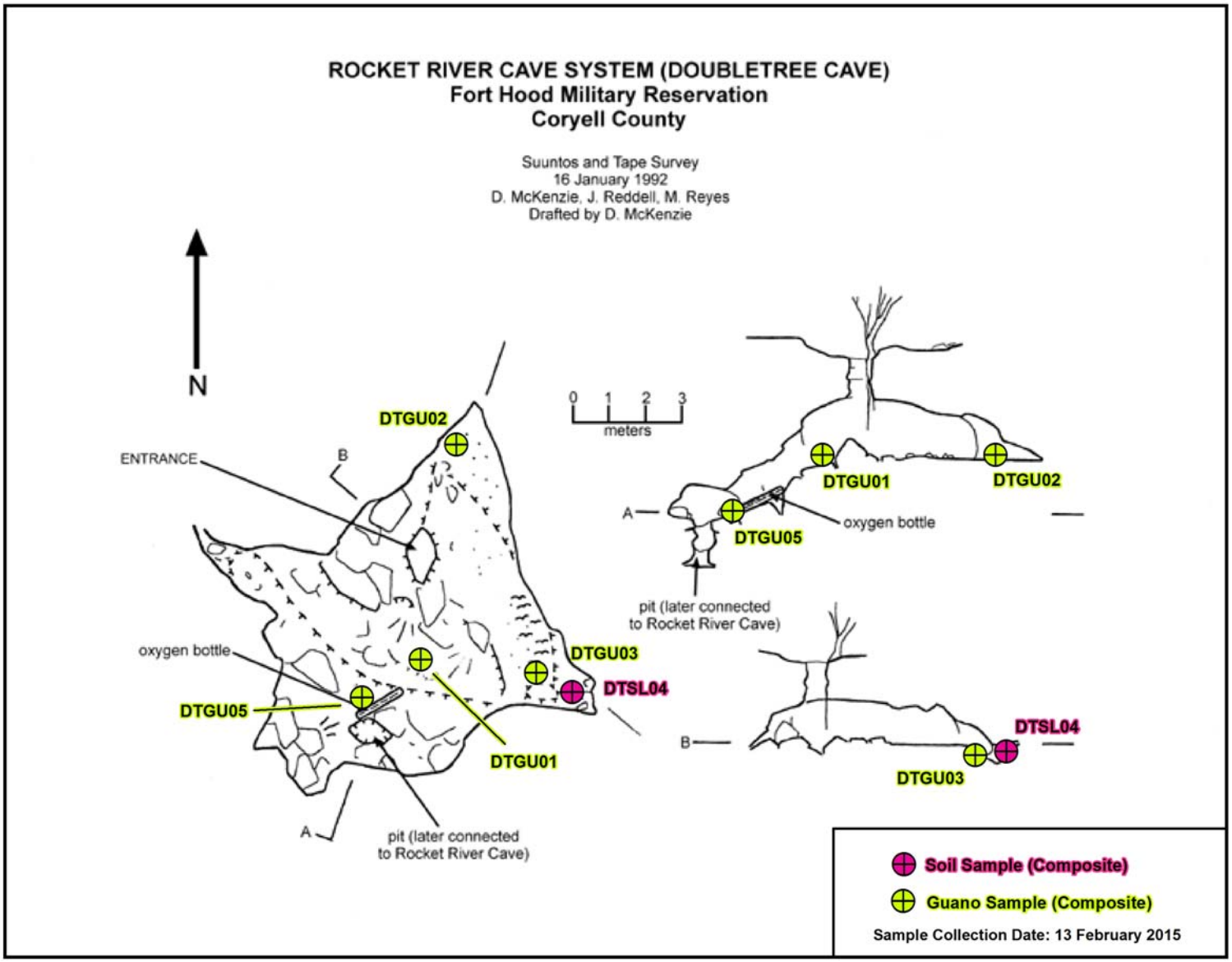

Figure 6. Plan and profile map of Doubletree Cave, showing sampling locations for various types of substrate collected.

Egypt Cave

Egypt Cave (Figure 8 and Figure 9) once housed a relatively large population of cave myotis (likely less than 33,000 individuals; Pekins 2012). The cave is now mostly unused by cave myotis, and low numbers (approximately 10 to 15) of tri-colored bats occupy it in the winter (Pekins 2012). There are two known primary roosts, located in two of the main rooms, with stained ceilings and accumulated guano mounds (Figure 7). Much of the cave passages are covered in loose, dark clay and clay loam, although many cave walls and floors consist of compacted claystone. Tree roots are evident along the ceilings of many rooms and passages and especially in two areas of the primary cave passage where two, separate, large tree roots have grown down from the surface and into the floor of the cave and essentially function as an extension of the trunks. Other organic material (e.g., leaf litter, dried grass and other forbs, scat, and wood) is distributed throughout the cave, although it is mostly concentrated around the cave's two entrances, which provide generally unrestricted airflow and good ventilation. Surface water from precipitation events does not reach all areas of the cave (e.g., the far reaches of joint passages) from the entrances, but it flows through much of the cave including the two rooms that house the known roosts. The cave entrance, situated on a mesa ridge overlooking the western portion of Fort Hood, is surrounded by woodland or brushland communities in various stages of succession from previous wildfires. A recent wildfire burned most of the woody vegetation surrounding the immediate vicinity of the entrance, although some isolated stands of trees and brush remain nearby.

Figure 7. Guano pile near sampling location EGGU08 in Egypt Cave.

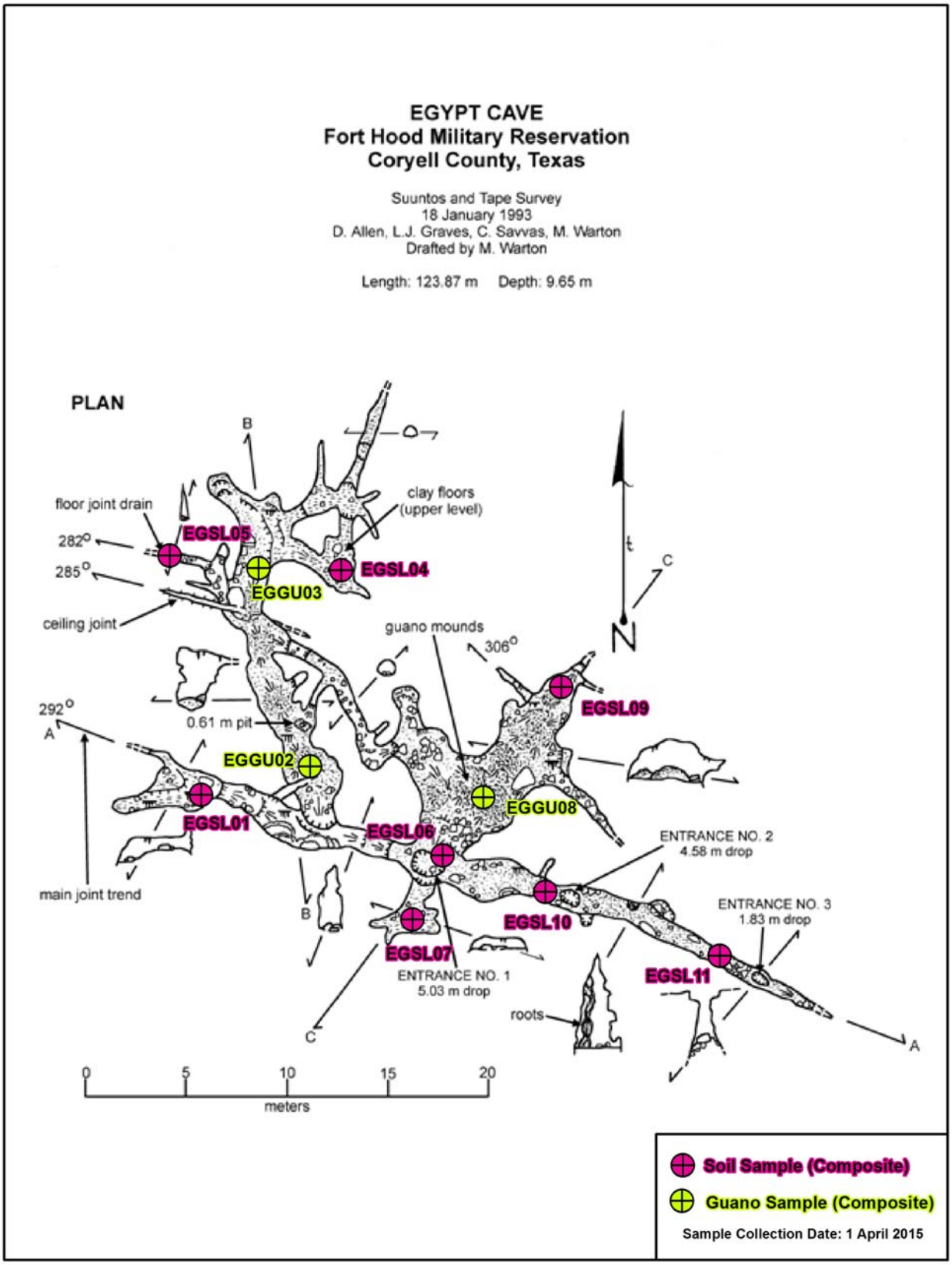

Figure 8. Plan map of Egypt Cave, showing sampling locations for various types of substrate collected.

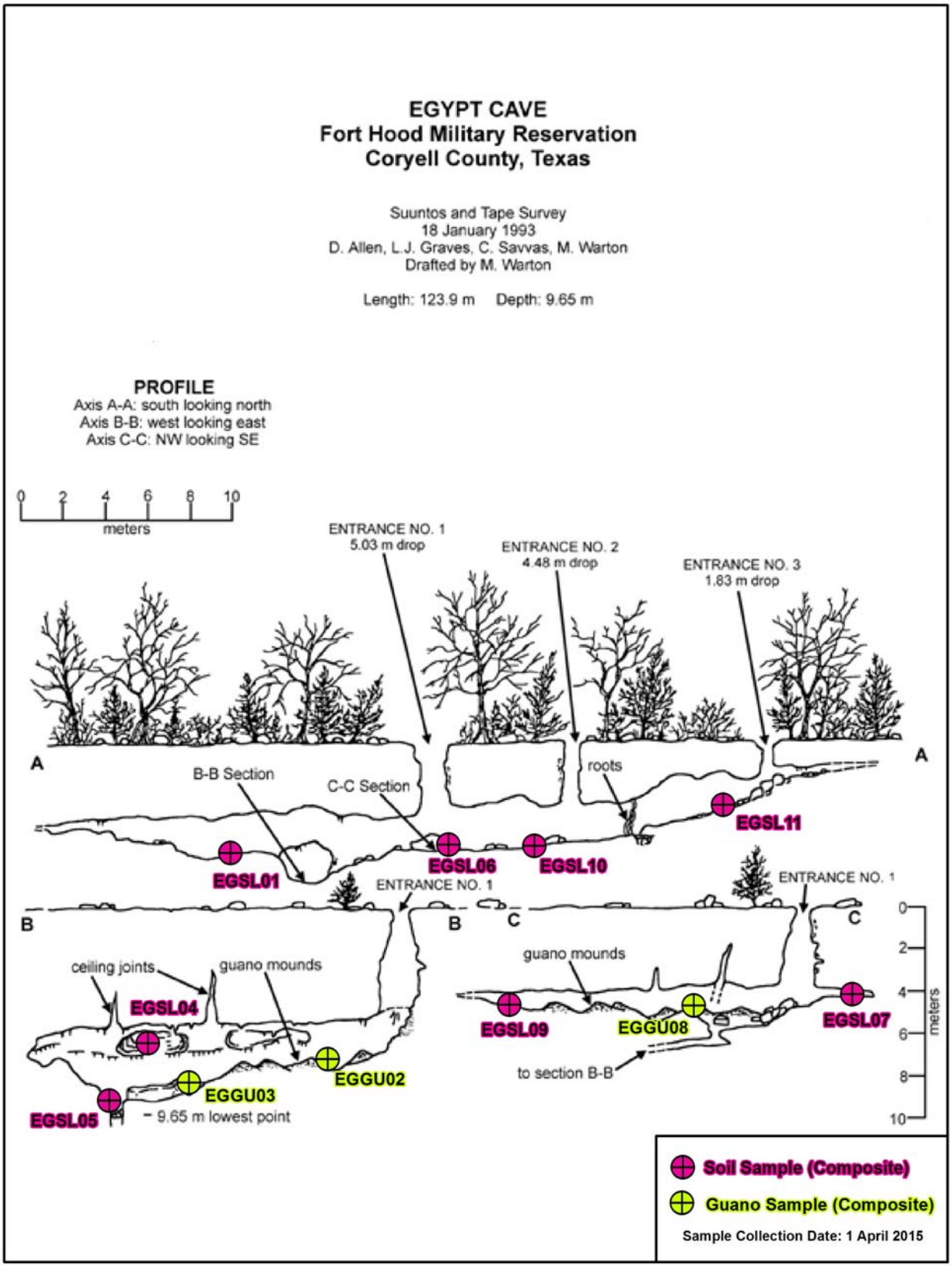

Figure 9. Profile map of Egypt Cave, showing sampling locations for various types of substrate collected.

Sample Collection Methods

Early site identification work occurred in December 2014 at Shell Mountain and Tippit caves during reconnaissance surveys; early reconnaissance did not occur at Doubletree and Egypt caves. During February and April of 2015, a team of two to four crewmembers conducted one sampling event at each of the four caves. Field scientists at least one staff member from Zara Environmental LLC (Zara) staff (Krista McDermid and Barrett Clark) and at least one staff member from the U.S. Army Garrison – Fort Hood, Environmental Division, Natural Resources Management Branch (Charles Pekins and Marion Noble). Before and after entering the study caves, all crewmembers followed the most recent set of National WNS Decontamination Protocols (version 6.25.2012; most recent protocols available for download at https://www.whitenosesyndrome.org/topics/decontamination).

We established sampling locations within each cave based on a variety of factors including selecting areas with a suitable amount of media for sampling; an adequate distribution of samples based on cave size, formation, and substrates; and specific areas of interest such as directly below or on known roosts, areas of differential temperature gradients, within flowpaths of water, or locations of visible fungal growth. The field crew established stations at each sampling location for repetitive sampling for future studies. Based on the sampled media, each station was color-coded using fluorescent nylon cable ties and marked tags for in-cave visibility and ease of reference (Figure 10). The field crew also photographed each station and recorded information about the general location, station-specific sampling procedures, or other local characteristics.

Figure 10. Labeled sampling location indicating that this sample was from Egypt Cave (EG), that the substrate collected was guano (GU) and that this was sample number 8.

We incorporated two sample suites in our study: a primary suite of collected media (e.g., soil and guano) at all four study caves and a secondary suite of swabbed substrates at SMBC. The swabbed samples at SMBC were collected for inclusion into a parallel study being conducted by Bat Conservation International in order to monitor for Pd in Texas caves known to contain hibernacula and/or maternity colonies of cave myotis and tri-colored bats.

In order to capture the greatest possible diversity of fungal material within a given area, the field crew composited samples during collection except as noted below. Thirty-five composite samples were collected using dedicated, clean gloves from within an approximate 1- to 2-m radius of each station, depending on the availability of sampled media at each location. The composite samples consisted of several subsamples that were mixed together to create one sample for analysis. In addition to the composite samples, three discrete samples were collected of a specific target, such as selecting a dead animal or material from a specific area of interest (e.g., visible fungal growth on a cave wall). We collected an additional suite of 30 samples in SMBC in February 2015 for the detection of *Pd* using alternative sampling and laboratory methods. We collected the additional suite of samples from walls and roost areas using the environmental (swab) sample collection protocol developed by the USGS NWHC (2014; Appendix). Figure 1, Figure 2, Figure 4, Figure 6, Figure 8, and Figure 9 present the locations of the sampling stations and type of sampled media in each of the four caves.

All samples were transported from the field in coolers containing ice or freezer-packs and held overnight in a freezer at 4°C or colder. The following day, the samples were shipped in coolers

containing freezer-packs via overnight delivery to the analytical laboratories. The primary suite of samples was sent to the Veterinary Diagnostic Laboratory at the University of Illinois at Urbana-Champaign (VDL), and the secondary suite of samples was sent to the U.S. Geological Service (USGS) National Wildlife Health Center (NWHC) Diagnostic Microbiology Laboratory (DML) in Madison, Wisconsin. The collected samples were held by the laboratories at -80°C until ready for further analysis.

Pd Screening Methods

For the secondary sample suite, the NWHC MDL used the protocol described in Muller et al. (2013). The methods described in Muller et al. (2013) established a sensitive, real-time, rapid PCR test for *Pd* that targets the intergenic spacer (IGS) region of the 18S rRNA gene complex. The IGS region, due to its high copies per fungal genome and its interspecific sequence variability, offers effective species- and subspecies-level sensitivity (Hillis and Dixon 1991; Jackson et al. 1999; Boyle et al. 2004; Muller et al. 2013). The collected material on the swabbed samples was used for the starting DNA material for PCR amplification.

For the primary sample suite, the VDL processed approximately 150 to 200 mg of sample material (e.g., guano, soil) for DNA extraction using the QIAamp® DNA Stool Mini Kit (Qiagen, Hilden, Germany) according to the manufacturer's instructions. The SurePrep™ Soil DNA Isolation Kit BP2815-50 (Fisher Scientific International, Inc., Hampton, New Hampshire) was used as an alternative, according to the manufacturer's instructions, for samples that were problematic (i.e., low yield) using the QIAamp® DNA Stool Mini Kit. The isolated DNA samples were held at -80°C until ready for PCR amplification.

The isolated DNA was used for PCR amplification of the 18S rRNA IGS region using two different sets of primers described in Muller et al. (2013) and synthesized by Integrated DNA Technologies (Coralville, IA): nu-IGS-0033-5'-Gd (sequence: 5'– TCT CCC ATT AAC TTG CAG GCT AG –3') paired with nu-IGS-0235-3'-Gd (sequence: 5'– ACC ACC GGC TCG CTA GGT A –3') for the production of an amplicon (PCR amplification product) that is 246 nucleotides (nt) long, and nu-IGS-0169-5'-Gd (sequence: 5'– TGC CTC TCC GCC ATT AGT G –3') paired with nu-IGS-0235-3'-Gd for a 100-nt long amplicon. A 190-µL (10X) PCR master reaction mix was created, consisting of 40 µL of 5X Phusion® HF buffer #F-518, 4.0 µL of a 10 mM dNTP mix (each nt), and 2.0 µL of Phusion® High Fidelity DNA Polymerase #F530S from New England BioLabs (Ipswich, MA); 5 µL of each 10 µM paired primer (nu-IGS-0033-5'-Gd/nu-IGS-0235-3'-Gd or nu-IGS-0169-5'-Gd/nu-IGS-0235-3'-Gd); and 134 µL of sterile double-distilled water. Final PCR reactions consisted of 19 µL of the above master mix and 1 µL of DNA. The thermal cycling profile used for amplification included an initial denaturation step at 98°C for 2 minutes followed by 30 cycles of 10 seconds of denaturation at 98°C, 30 seconds of annealing at 54°C, and 30 seconds of elongation at and 72°C. The amplification was terminated by a final extension of 72°C for 10 minutes. Upon completion, the amplicons were held at 4°C until ready for denaturing gradient gel electrophoresis (DGGE). The amplicons were run on 2 percent agarose gels at 150V for 50 minutes. Depending on the executed primer(s), the production of the appropriate size band (e.g., 246 nt, 100 nt) confirmed the presence of *Pd* DNA

in the sample (or other genetic target, such as control samples; see below). The resulting bands were excised from the agarose gels, and DNA was isolated from the excised bands using Qiaquick Gel Extraction Kit (Qiagen, Gaithersburg, Maryland) according to the manufacturer's instructions. The extracted DNA samples were held at -80°C until ready for PCR amplification for the characterization of fungal taxa (described below).

For the primary sample suite, amplified samples were tested for quality DNA isolation by the presence of short 16S rRNA gene primers for general bacterial DNA (rrs). Additional quality controls, including the use of mitochondrial rRNA primers (16Smt) and internal transcribed spacer (ITS; discussed below) region primers (ITS3 and ITS4; White et al. 1990), tested for the presence of a broad range of fungal taxa. To test for inhibition, samples were spiked with *Pd* DNA or other genetic targets (depending on quality control primers) to be analyzed as positive control samples. Negative controls lacking genetic target material were also included. The control samples were analyzed by the respective methods as described above.

Fungal Community Detection Methods – Molecular

The VDL provided a characterization of fungal communities by utilizing two internal transcribed spacer (ITS) primers: ITS4 and ITS5 (White et al. 1990). Although using the ITS region for phylogenetic studies has drawbacks (Ferliner and Rosselló 2007), it is one of the most widely sequenced regions of fungal DNA, and it is currently understood to present the highest probability of successful identification for the widest range of fungal taxa (Schoch et al. 2012). The previously extracted DNA (primary sample suite) was used for PCR amplification of the ITS I region of the fungal 18S rRNA gene using ITS4 and ITS5 PCR primers (ITS4 sequence: 5'– TCC GCT TAT TGA TAT GC –3'; ITS5 sequence: 5'– GGA AGT AAA AGT CGT AAC AAG G –3'), as synthesized by Integrated DNA Technologies (Coralville, IA). A 50-µL PCR reaction mix consisted of one OmniMix HS lyophilized bead (Cepheid, Sunnyvale, CA), a concentration of 500 nM for each of the PCR primers, and DNAse- and RNAse-free water (Thermo Fisher Scientific, Grand Island, NY). Final PCR amplification for each sample consisted of 23 µL of the above master mix and 2 µL of each isolated sample DNA (approximately 200 ng). The thermal cycling profile used for amplification included an initial denaturation step at 95°C for 2 minutes followed by 30 cycles of 1 minute of denaturation at 95°C, 1 minute of annealing at 55°C, and 1 minute of elongation at and 72°C. The amplification was terminated by a final extension of 72°C for 10 minutes. Upon completion, the amplicons were held at 4°C until ready for DGGE.

The amplicon samples were loaded and run on 2 percent agarose gels at 150V for 50 minutes to determine successful amplification. The DGGE bands were evaluated to assess the quality of DNA based on intensity. Individual bands exhibiting the greatest intensity in each sample were selected to represent the target genetic material for sequencing (i.e., not all of the successfully amplified genetic material in each amplicon sample was selected for further analysis). The selected bands were excised from the agarose gels, and DNA was isolated from the excised gel fragment using Qiaquick Gel Extraction Kit (Qiagen, Gaithersburg, Maryland) according to the manufacturer's instructions. The DNA isolated from the excised bands was eluted in 25 to 30 µL

of DNAse- and RNAse-free water and sequenced with ITS4 and ITS5 primers. The forward and reverse sequence reads were assembled using an automated sequencer. The sequence homology analysis was performed using the basic local alignment search tool for nucleotides (BLASTn) standard algorithm (National Center for Biotechnology Information, Bethesda, MD) to compare nucleotide query sequences against the GenBank nucleotide sequence database for tentative identifications based on sequence similarity. For each queried sequence, tentative identifications to the lowest taxonomic rank were based on the BLASTn sequence results with the highest matching percentage and a statistically significant E value (expectation value) of less than 10^{-4}.

Fungal Community Detection Methods – Culturing

The VDL included an alternative analysis for the detection of fungal taxa using a culturing methodology. The identities of cultured isolates were verified using either matrix-assisted laser desorption/ionization (MALDI) time of flight (TOF) mass spectrometry or PCR for sequencing 18S gene amplicons. Field-collected samples (primary sample suite) were plated in the first quadrant of three agar plates consisting of Sabouraud dextrose (Remel 01760), Sabouraud dextrose with chloramphenicol (Remel 01770), and Sabouraud dextrose with chloramphenicol and cyclohexamide (Remel 01776). Plates were inoculated with sample material and incubated at 25 to 28°C for at least 30 days. Once incubated, the inoculated plates were inspected weekly. Active colonies were sub-cultured for purity as well as to prevent overgrowth by other organisms. Lacto-phenol cotton blue staining was performed to examine microscopic morphology to aid in identification. Sabouraud broth subcultures were inoculated using advancing hyphae along the margin of colonies and incubated on a rotator for 1 to 5 days until turbid. Pellets were created from the turbid broth (containing fungal growth) using a centrifuge and the pellets were triple washed using high performance liquid chromatography water, followed by an ethanol wash, and dried. The pellet was resuspended in 10 to 100 µL of 70 percent formic acid with an equal part acetonitrile and vortexed for two minutes. A 1-µL aliquot of the vortexed solution was placed on a stainless steel MALDI Biotyper template to dry, after which 1 µL of α-cyano-4-hydroxycinnamic acid peptide matrix is added and again allowed to dry. A Bruker® MALDI-TOF Biotyper was used for identification of the dried sample material. Organisms that were not clearly identified using the MALDI-TOF were submitted for 18S rRNA gene sequencing using the molecular methods as described above.

Microclimate Data Collection Methods

Microclimate data collection followed the methodology described by Pekins (2012). In summary of Pekins (2012), Hobo Pro H08-32-08 datalogger sensors (Onset Computer Corporation) collected long-term surface and cave microclimate data, including temperature and absolute humidity (AH), every 1.5 hours. Pekins (2012) accessed in-cave datalogger sensors each winter to avoid disturbing bats occupying the caves during the warmer months. In addition to the datalogger stations, the author collected ceiling temperatures, the temperature of hibernating bat bodies, and adjacent roost temperatures using a Raytex Raynger ST Pro infrared laser

thermometer (Fluke Company) and relative humidity at the midpoint between the cave floor and ceiling using a Kestrel 3500 handheld weather meter (Nielson-Kellerman Company).

Results

We collected 38 samples of guano, soil, and two carcasses (bat, mouse) among the four study caves on 04 February 2015, 13 February 205, and 1 April 2015 (primary sample suite). The sampled areas included mounds of fresh guano, identified by the presence of loose, rod-shaped excrement, and older guano mounds that were relatively dry and stable. Some samples included loose soil (typically loamy or clayey) or sediment, some of which mixed with organic material (leaves, whole seeds and seed shells, twigs, visible hyphae). Other soil samples consisted of compacted clay, some with a thin, overlying layer or dusting of old guano. We collected an additional 30 swab samples from the ceilings and walls in SMBC on 04 February 2015 for the detection of the presence of *Pd* using alternative laboratory methods (secondary sample suite). Figure 1, Figure 2, Figure 4, Figure 6, Figure 8, and Figure 9 present the locations of the sampling stations and type of sampled media in each of the four caves.

Pd Screening Results

Amplicons from all of the samples in the primary and secondary suites resulted in negative detections of *Pd* by their respective molecular analysis methodology. A discussion of the quality control samples is included below. The results of the *Pd* screening and sample quality control analysis are presented in Table 1.

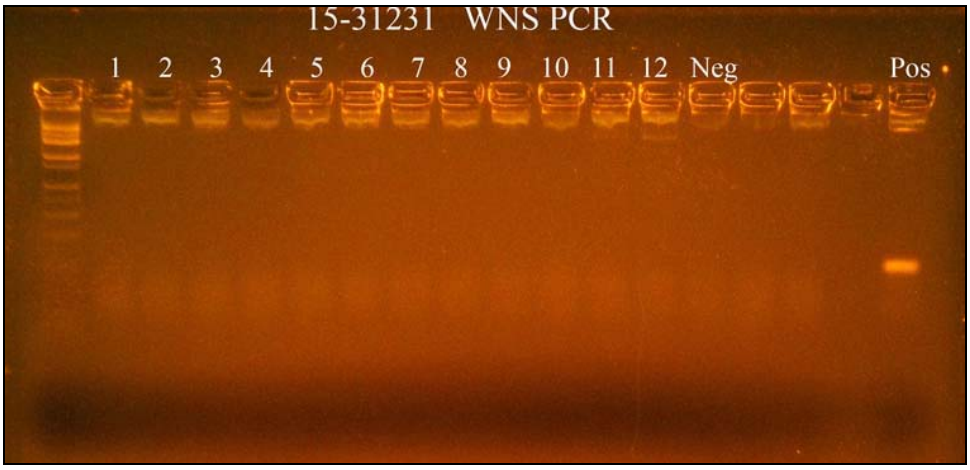

Figure 11. Negative detection of *Pd* in a representative laboratory DGGE sample set correlating with the results from 09 June 2015 (presented in Table 1). The nucleotide reference ladder is located in the far left lane, while the *Pd* screening test samples are located in Lanes 1 through 12. The lanes labeled “Neg” and “Pos” are the negative and positive controls, respectively.

With the exception of laboratory sample 15-33184-11 (field sample TPSL05), confirmation of quality DNA isolated from both the QIAamp® DNA Stool Mini Kit and SurePrep™ Soil DNA Isolation Kit BP2815-50 was achieved for all samples by the use of the general fungal primers (ITS3 and ITS4) and general bacterial primers (16S rrs). Samples isolated with the stool kit and tested for quality using the rrs primers resulted in a 20.4% detection rate of the genetic target (including the positive and negative control samples). Most of the non-detections using samples isolated with the stool kit occurred in the 15-31687 (Doubletree and Tippit caves) and 15-33184 (Egypt Cave) laboratory sample sets. Reanalyzing the DNA isolated using the soil kit resulted in an improved genetic target detection rate of 52.9% (including the positive and negative controls). Using the ITS3 and ITS4 primers, the genetic target, including the positive and negative controls, was detected at a similar rate for both kits (49.0% for the stool kit and 47.1% for the soil kit).

Three negative detections occurred in the positive control samples (15-31687 sample set, 22 April 2015, ITS3/4 primers; 15-31687 sample set, 15 May 2015, 16S rrs primers; 15-33184 sample set, 15 May 2015, 16S rrs primers) using the DNA isolated with the stool kit. In addition, four weak positive detections occurred in the negative controls using both the stool kit (15-31231 sample set, 21 April 2015, ITS3/4 primers) and soil kit (15-31231 sample sets, 19 May 2015, 16S mt primers; 15-31687 sample set, 16S mt primers, 19 May 2015; 15-33184 sample set, 16S mt primers, 09 June 2015). For quality control, sample sets with erroneous positive or negative control results were re-analyzed. Quality control was ultimately achieved in both the positive and negative controls for the final *Pd* screening results.

Table 1. Results of the Pd screening analysis including quality control results.

QIAGEN Stool Prep (DNA Isolation 4/20/2015)						SurePrep Soil Prep (DNA Isolation 5/18/2015)				
	PCR Analysis (Analysis Date)						PCR Analysis (Analysis Date)			
Lab Sample ID	*Pd* (4/20/15)	16S (mt) (4/21/15)	ITS3/4 (5/11/15)	16S (rrs) (5/15/15)	*Pd* (6/9/15)	Lab Sample ID	ITS3/4 (5/18/15)	16S (mt) (5/19/15)	*Pd* (5/19/15)	16S (rrs) (5/20/15)
15-31231 1	-	+	+	-	NM	15-31231 1	NM	NM	NM	NM
15-31231 2	-	+	-	+	NM	15-31231 2	NM	NM	NM	NM
15-31231 3	?	+	+	+	-	15-31231 3	NM	NM	NM	NM
15-31231 4	-	-	-	-	NM	15-31231 4	+	+	-	-
15-31231 5	-	+	+	-	NM	15-31231 5	NM	NM	NM	NM
15-31231 6	-	+	+	-	NM	15-31231 6	NM	NM	NM	NM
15-31231 7	-	-	+ (1:10)*	-	NM	15-31231 7	NM	NM	NM	NM
15-31231 8	-	+	+	-	NM	15-31231 8	NM	NM	NM	NM
15-31231 9	-	+	+	+	NM	15-31231 9	NM	NM	NM	NM
15-31231 10	-	-	-	-	NM	15-31231 10	+	+	-	+
15-31231 11	-	+	+/-	+	NM	15-31231 11	NM	NM	NM	NM
15-31231 12	-	+	+/-	+	NM	15-31231 12	NM	NM	NM	NM
Negative Control	-	+/-	-	-	-	Negative Control	-	+/-	-	-
Positive Control	+	+	+	+	+	Positive Control	+	+	+	+

QIAGEN Stool Prep (DNA Isolation 4/21/2015)					SurePrep Soil Prep (DNA Isolation 5/18/2015)				
	PCR Analysis (Analysis Date)					PCR Analysis (Analysis Date)			
Lab Sample ID	ITS3/4 (4/22/15)	*Pd* (5/13/15)	16S (rrs) (5/15/15)	ITS3/4 (6/9/15)	Lab Sample ID	ITS3/4 (5/18/15)	16S (mt) (5/19/15)	*Pd* (5/19/15)	16S (rrs) (5/20/15)
15-31687 1	-	-	-	NM	15-31687 1	-	+	-	+
15-31687 2	-	-	-	NM	15-31687 2	-	+	-	+
15-31687 3	+	-	-	NM	15-31687 3	+	+	-	-
15-31687 4	+	-	-	NM	15-31687 4	+	+	-	+
15-31687 5	-	-	-	+	15-31687 5	-	+	-	-
15-31687 6	+	-	-	NM	15-31687 6	+	+	-	+
15-31687 7	-	-	-	NM	15-31687 7	+	+	-	-
15-31687 8	+	-	-	+	15-31687 8	-	+/-	-	-
15-31687 9	-	-	-	+	15-31687 9	-	+	-	-
15-31687 10	+	-	+	NM	15-31687 10	+	+	-	+
15-31687 11	-	-	-	-	15-31687 11	-	+/-	-	-
15-31687 12	+	-	-	+/-	15-31687 12	-	+	-	-
15-31687 13	+	-	+	NM	15-31687 13	-	+/-	-	-
15-31687 14	+	-	-	NM	15-31687 14	+	+	-	+
15-31687 15	-	-	-	NM	15-31687 15	+	+	-	+
Negative Control	-	-	-	-	Negative Control	-	+/-	-	-
Positive Control	-	+	-	+	Positive Control	+	+	+	+

QIAGEN Stool Prep (DNA Isolation 4/23/2015)					SurePrep Soil Prep (DNA Isolation 5/22/2015)					
	PCR Analysis (Analysis Date)					PCR Analysis (Analysis Date)				
Lab Sample ID	*Pd* (4/23/15)	ITS3/4 (4/23/15)	*Pd* (5/13/15)	16S (rrs) (5/15/15)	Lab Sample ID	ITS3/4 (5/22/15)	ITS3/4 (6/9/15)	16S (mt) (6/9/15)	*Pd* (6/9/15)	16S (rrs) (6/10/15)
15-33184 1	-	+	-	+	15-33184 1	-	-	-	-	-
15-33184 2	-	+	-	-	15-33184 2	-	-	-	-	+/-
15-33184 3	-	-	-	-	15-33184 3	-	-	-	-	+
15-33184 4	-	+	-	-	15-33184 4	-	-	+	-	-
15-33184 5	-	-	-	-	15-33184 5	-	-	-	-	+
15-33184 6	-	-	-	-	15-33184 6	+	+	+	-	+
15-33184 7	-	+	-	-	15-33184 7	-	-	-	-	-
15-33184 8	-	+	-	-	15-33184 8	+	+	+	-	+
15-33184 9	-	+	-	-	15-33184 9	-	-	-	-	-
15-33184 10	-	-	-	-	15-33184 10	+	+	+	-	+
15-33184 11	-	-	-	-	15-33184 11	+	+	+	-	+
Negative Control	-	-	-	-	Negative Control	-	-	+/-	-	-
Positive Control	+	+	+	-	Positive Control	+	+	+	+	+

+ = Positive detection
- = Negative detection
+/- = Weak positive detection
? = Questionable detection
NM = Not measured/analyzed
*Attempted template dilution ratio used to achieve successful amplicon due to inhibitor in sample.

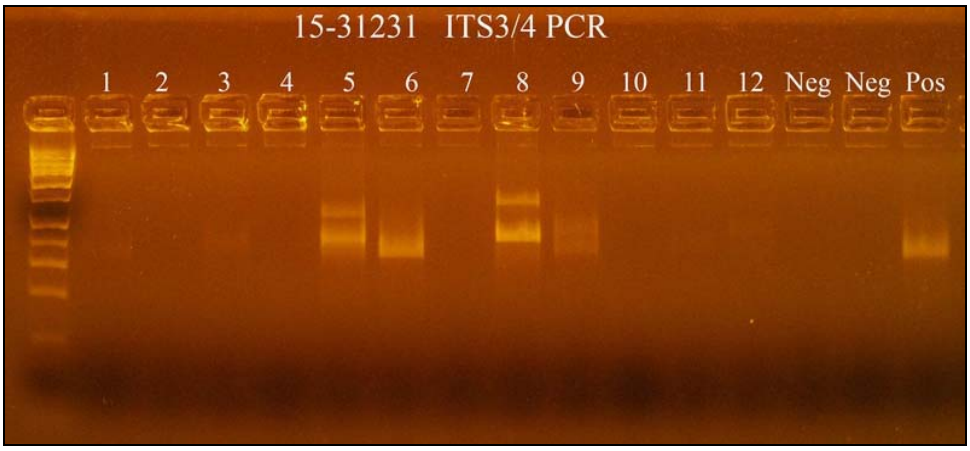

Figure 12. Amplification results using ITS3/4 PCR in a representative laboratory DGGE sample set correlating with the results from 11 May 2015. The nucleotide reference ladder is located in the far left lane, while the ITS3/4 amplicon samples are located in Lanes 1 through 12. The lanes labeled "Neg" and "Pos" are the negative and positive controls, respectively.

Fungal Community Detection Results

Providing a representative set of sampled locations among the four study caves, 14 of the previously isolated DNA samples (described above) from the primary sample suite were used for the characterization of fungal communities using ITS4/ITS5 methodology. Eight of the field-collected samples (primary suite) were included in the analysis for the detection of fungal taxa using culturing methodology. One of the eight cultured samples (TPSL02) was not included in the analysis using the ITS4/ITS5 PCR methods described above. The results of the ITS4/ITS5 PCR methodology are presented in Table 2. The results of the culturing methodology are presented in Table 3.

Table 2. Fungal taxa identified using ITS4/ITS5 PCR methodology

Lab Sample ID	Field Sample ID	Date of Extraction	Extraction Kit	ITS4/ITS5 Amplicon Production	Sequence Result Comment	ITS4 Primer			ITS5 Primer		
						Matching Nucleotide Alignment (ntSample/ ntGenBase)	Percent Nucleotide Homology	Best Homology Match (GenBank EMBL ID)	Matching Nucleotide Alignment (ntSample/ ntGenBase)	Percent Nucleotide Homology	Best Homology Match (GenBank EMBL Id)
Shell Mountain Bat Cave Samples											
15-31231-6	SMGU05	4/20/2015	Stool prep	Positive	Good Sequence	572/575	99	*Chaetomium* sp. (HQ832964.1)	558/561	99	*Chaetomium* sp. (HQ832964.1)
15-31231-7	SMGU06	5/11/2015	Stool prep	Positive (1:10)*	Bad Sequence	NM	NM	NM	NM	NM	NM
				Positive; 2 bands (1:100)*	Bad Sequence	NM	NM	NM	NM	NM	NM
15-31231-2	SMGU02	4/20/2015	Stool prep	Weak Positive	--	NM	NM	NM	NM	NM	NM
15-31231-3	SMBT01	4/20/2015	Stool prep	Positive	Bad Sequence	NM	NM	NM	NM	NM	NM
Doubletree Cave Samples											
15-31687-3	DTGU03	4/21/2015	Stool prep	Positive	--	541/546	99	*Chaetomidium arxii* (LN809035.1)	534/552	97	*Chaetomium* sp. (EU750691.1)
15-31687-4	DTSL04	4/21/2015	Stool prep	Negative	--	NM	NM	NM	NM	NM	NM
Tippit Cave Samples											
15-31687-7	TPSL01	5/18/2015	Soil prep	Positive	--	479/488	98	*Trichosporon smithiae* (NR_073230.1)	501/514	97	*Trichosporon smithiae* (NR_073230.1)
15-31687-11	TPSL05	4/11/2015	Stool prep	Negative	--	NM	NM	NM	NM	NM	NM
15-31687-6	TPMS01	4/21/2015	Stool prep	Positive	Noisy Sequence	431/494	87	*Chrysosporium vallenarense* (AJ390389.1)	275/324	85	*Chrysosporium vallenarense* (AJ390389.1)
Egypt Cave Samples											
15-33184-3	EGGU03	5/22/2015	Soil prep	Positive	Bad ITS5 Sequence	359/400	90	*Penicillium* sp. (AY354257.1);	NM	NM	NM
						328/368	89	*Aspergillus fumigatus* (HG798742.1)	NM	NM	NM
						448/505	89	*Penicillium parviverrucosum* (KP119477.1)	507/581	87	*Penicillium* sp. (KJ174314.1)
15-33184-8	EGGU08	4/22/2015	Stool prep	Positive	Good Sequence	538/587	92	*Phialosimplex salinarum* (KF274690.1)	535/584	92	*Phialosimplex salinarum* (KF274692.1)
15-33184-9	EGSL09	4/22/2015	Stool prep	Positive	Bad ITS5 Sequence	505/555	91	*Phialosimplex chlamydosporus* (GQ169326.1)	NM	NM	NM
				Positive (1:10)*	Noisy Sequence	480/515	93	*Phialosimplex chlamydosporus* (GQ169326.1)	559/600	93	*Phialosimplex chlamydosporus* (GQ169326.1)
15-33184-4	EGSL04	4/22/2015	Stool prep	Weak Positive; 2 bands	NM	NM	NM	NM	NM	NM	NM
15-33184-1	EGSL01	4/22/2015	Stool prep	Positive; 2 bands	NM	NM	NM	NM	NM	NM	NM

NM = Not measured, either due to weak/no amplicon production or bad sequencing results
*Attempted template dilution ratio used to achieve successful amplicon due to inhibitor in sample.

Table 3. Fungal taxa identified using culturing methodology.

Cultured From Lab Sample ID (Field Sample ID)	Isolate ID	Population Growth	Fungal ID	Isolate Identification Method
Shell Mountain Bat Cave Samples				
15-31231-7 (SMGU06)	71	Moderate	Uncultured fungus closest to *Gleotinia*	18S PCR
	72	Moderate	*Blastobotrys* sp.	18S PCR
	73	Rare	*Alternaria alternata*	MALDI - ED
	74	Overgrowth	*Mucor* sp.	MALDI - ED
	75	Rare	*Fusarium*	MALDI - ED
	76	Rare	*Curvularia*	MALDI - ED
	83	Rare	*Trichosporon laibachii*	MALDI - FE
15-31231-3 (SMBT01)	77	Few	Uncultured fungus closest to Hypocreales	18S PCR
	78	Moderate	*Chrysosporium*	18S PCR
	79	NA	*Blastobotrys* sp.	Visual = Isolate 72
	80	Heavy	*Penicillium* sp.	MALDI - ED
	86	Heavy	*Aspergillus sclerotiorum*	MALDI - ED
	88	Very light	*Chrysosporium*	18S PCR
Doubletree Cave Samples				
15-31687-3 (DTGU03)	79	Overgrowth	*Mucor* sp.	MALDI - ED
	80	Heavy	*Penicillium* sp.	18S PCR
	81	Moderate	*Villosiclava* sp., *Fusarium* sp., *Ustilaginoidea* sp.	18S PCR
Tippit Cave Samples				
15-31687-7 (TPSL02)	71	Overgrowth	*Mucor* sp.	MALDI - ED
	72	Moderate	*Penicillium* sp.	MALDI - ED
	73	Light	*Ustilaginoidea* sp., *Verticillium* sp., *Coniella* sp.	18S PCR
15-31687-6 (TPMS01)	76	Rare	Bionectriacea, *Clonostachys* sp.	18S PCR
	78	Rare	*Trichosporon laibachii*	MALDI - ED
	79	Heavy	*Chrysosporium* sp., *Shanorella* sp.	18S PCR
Egypt Cave Samples				
15-33184-8 (EGGU08)	71	Very rare	*Penicillium chrysogenum*	18S PCR
	72	Very rare	*Malbranchea flava*, *Auxarthron ostraviense*	18S PCR
	73	Very few	*Penicillium brevicompactum*	18S PCR
	74	Very rare	*Geomyces* sp., *Ciliciopodium hyalinum*	18S PCR
	75	Very rare	*Pseudogymnoascus* sp.	18S PCR
			Geomyces sp.	18S PCR (WNS primers)
15-33184-9 (EGSL09)	77	Few	NA	18S PCR
	78	Rare	*Penicillium* sp.	18S PCR
	79	Very rare	NA	18S PCR
	80	Very rare	NA	18S PCR
	81	Rare	NA	18S PCR
	82	Very rare	*Paecilomyces lilacinus*	MALDI – FE
	83	Very rare	*Wardomycopsis humicola*	18S PCR
	84	Very rare	*Penicillium brevicompactum*	MALDI – FE

MALDI – ED = Matrix-assisted laser desorption/ionization (Edman degradation) mass spectrometry technique
MALDI – FE = Matrix-assisted laser desorption/ionization (field emission) mass spectrometry technique
18S PCR = PCR amplification of the ITS I region of the fungal 18S rRNA gene using ITS4 and ITS5 PCR primers (unless noted)
NA = Not available due to bad sequence

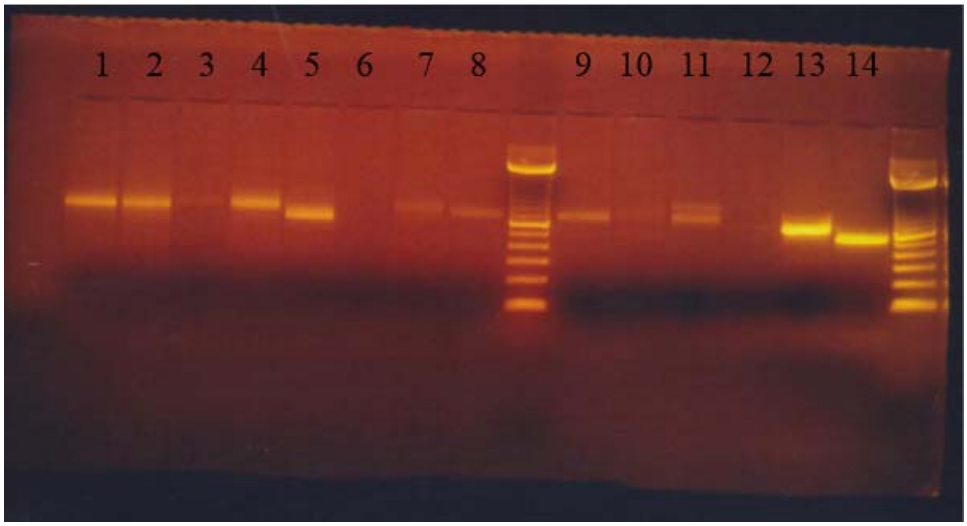

Figure 13. Amplification results using ITS5/5 PCR in a representative laboratory DGGE sample set correlating with the "ITS4/ITS5 Amplicon Production" column presented in Table 2. Lane 12 is the negative control and lanes 13 and 14 are the positive controls. The nucleotide reference ladders are located between lanes 8 and 9 and in the far right lane, while the ITS4/5 amplicon samples are located in lanes 1 through 11 as follows: SMGU05, SMGU06, SMGU02, SMBT01, DTGU03, DTSL04, TPSL01, TPSL05, TPMS01, EGGU03, EGGU08, EGSL09, EGSL04, and EGSL01.

Microclimate Data Results

Table 4 through Table 7 present the microclimate data described in Pekins (2012), along with additional data collected by the author after 2012 using the same methodology. A summary of the data from Pekins (2012) and data collected after 2012 is provided below.

Among the three study caves with available microclimate data collected by the dataloggers (Table 4 through Table 6), SMBC exhibited the widest range of average temperatures. Between 2004 and 2014, the 10-year average air temperature of SMBC ranged from a low of 10.7°C (SD 1.1) to a high of 26.7°C (SD 1.3). The difference in average temperature at Tippit and Egypt caves was considerably lower for the 10-year data collection period. The range of average low and average high temperatures was a difference of only 1°C in Tippit Cave (18.2°C [SD 1.1] to 19.2°C [SD 0.87]) and 3.1°C in Egypt Cave (14.6°C [SD 0.70] to 17.7°C [SD 0.78]). Average AH data showed similar trends among the three caves for the 10-year period, with a high of 25.1 g/m^3 (SD 2.2) and low of 4.6 g/m^3 (SD 5.2) in SMBC (a difference of 20.5 g/m^3) and much lower differences of humidity levels occurring in Tippit Cave (15.6 g/m^3 [SD 1.0] to 16.4 g/m^3 [SD 0.94] for a variance of 0.8 g/m^3) and Egypt Cave (12.5 g/m^3 [SD 0.55] to 15.2 g/m^3 [0.69] for a variance of 2.7 g/m^3).

Table 4. Datalogger microclimate recordings (lows and highs) Shell Bat Cave. Adapted from Pekins (2012).

Year	Low Temperature (°C)	High Temperature (°C)	Low Absolute Humidity (g/m^3)	High Absolute Humidity (g/m^3)
2004-2005	11.5	26.5	10.3	24.7
2005-2006	12.1	26.1	10.9	23
2006-2007	10.6	26.8	1.2	25.1
2007-2008	10.9	29.3	0.3	29.5
2008-2009	11.1	26.1	0.1	24.8
2009-2010	9	26.9	0.08	25.7
2010-2011	Unavailable	Unavailable	Unavailable	Unavailable
2011-2012	9.5	25.2	9.1	23.2
2012-2013	Unavailable	Unavailable	Unavailable	Unavailable
Mean (SD)	**10.7 (1.1)**	**26.7 (1.3)**	**4.6 (5.2)**	**25.1 (2.2)**
2013-2014	Unavailable	Unavailable	Unavailable	Unavailable

Table 5. Datalogger microclimate recordings (lows and highs) Tippit Cave. Adapted from Pekins (2012).

Year	Low Temperature (°C)	High Temperature (°C)	Low Absolute Humidity (g/m^3)	High Absolute Humidity (g/m^3)
2004-2005	18.7	19.5	16	16.7
2005-2006	19	19.9	16.3	17.2
2006-2007	19	19.9	16.3	17.1
2007-2008	Unavailable	Unavailable	Unavailable	Unavailable
2008-2009	Unavailable	Unavailable	Unavailable	Unavailable
2009-2010	16.5	17.9	13.9	15
2010-2011	Unavailable	Unavailable	Unavailable	Unavailable
2011-2012	17.9	18.7	15.3	15.8
2012-2013	Unavailable	Unavailable	Unavailable	Unavailable
Mean (SD)	**18.2 (1.1)**	**19.2 (.87)**	**15.6 (1)**	**16.4 (.94)**
2013-2014	Unavailable	Unavailable	Unavailable	Unavailable

Table 6. Datalogger microclimate recordings (lows and highs) Egypt Cave. Adapted from Pekins (2012).

Year	Low Temperature (°C)	High Temperature (°C)	Low Absolute Humidity (g/m^3)	High Absolute Humidity (g/m^3)
2005-2006	13.9	17.4	12.1	14.9
2006-2007	13.9	16.7	12	14.3
2007-2008	Unavailable	Unavailable	Unavailable	Unavailable
2008-2009	15.2	17.5	13	14.9
2009-2010	14.2	17.4	12.1	14.9
2010-2011	14.9	18.7	12.7	16
2011-2012	15.6	18.6	13.3	16
2012-2013	Unavailable	Unavailable	Unavailable	Unavailable
Mean (SD)	**14.6 (.7)**	**17.7 (.78)**	**12.5 (.55)**	**15.2 (.69)**
2013-2014	Unavailable	Unavailable	Unavailable	Unavailable

Table 7. Single visit December microclimate measurements. Adapted from Pekins (2012).

	Doubletree Cave	**Egypt Cave**	**Shell Mountain Bat Cave**	**Tippit Cave**
Year	**Mean Temperature °C (SD); Range**	**Mean Temperature °C (SD); range**	**Mean Temperature °C (SD); range**	**Mean Temperature °C (SD); range**
2006	19.2° (1.3°); 16.4° - 21.2°	17.7° (1.5°); 14.6° - 20.6°	17.2° (3°); 8.6° - 22.6°	19.9° (1.4°); 15.3° - 21.6°
2007	18.4° (1.1°); 16.8° - 20.3°	17.3° (2.5°); 12.56° - 21.4°	Not measured	20.1° (2°); 16° - 23.2°
2008	20.5° (1.3°); 18.6° - 22.4°	18.3° (1.8°); 14.2° - 21.9°	17° (2.8°); 9.4° - 22.6°	21.4° (1°); 17° - 22.6°
2009	18.2° (1.4°); 15.2° - 20.4°	17.8° (1.8°); 13.6° - 21.2°	16.4° (3.2°); 6.6° - 22.4°	19.8° (1.9°); 13.9° - 22.4°
2010	19.2° (1.2°); 17.6° - 21.2°	16.3° (1.6°); 13.4° - 19.6°	16.8° (2.9°); 8.4° - 22.8°	19.7° (1.1°); 16.4° - 21.6°
2011	18.5° (1.6°); 15.6° - 20.4°	16.5° (1.9°); 11.8° - 20.2°	17° (2.1°); 13° - 21.4°	19.3° (1.7°); 13.4° - 21.6°
2012	19.8° (1.3°); 17.4° - 21.8°	18.5° (1.4°); 16.2° - 21.6°	18.4° (2.3°); 13° - 23.2°	20.9° (1.2°); 15.6° - 22.8°
2013	19.1° (1.3°); 17.4° - 21.2°	16.3° (2.1°); 12.8° - 20.4°	15.6° (3.9°); .4° - 22.8°	20.7° (1.1°); 17.2° - 22.4°
2014	18.6° (1.6°); 15.8° - 20.6°	17.8° (1.9°); 14.2° - 21.4°	17.8° (1.7°); 15.4° - 21.4°	20° (1°); 17.6° - 21.8°
	Mean RH % (SD); Range	**Mean RH % (SD); Range**	**Mean RH % (SD); Range**	**Mean RH % (SD); Range**
2006	71.1 (4.2); 64 - 76.5	73.8 (4); 69 - 87.3	74 (9.9); 53 - 91.3	82 (3.9); 78.1 - 90.9
2010	67.8 - 85	78.7 (3); 75.4 - 83.8	73.1 (8.5); 59.5 - 92.1	82.7 (2.2); 80.1 - 85.8
2011	93.2 (7.6); 82.6 - 99.2	78.6 (6); 69.5 - 92.6	86.2 (6.9); 72.8 - 96.7	90.8 (7.5); 76.1 - 100
2012	79.6 (1.7); 78.4 - 82.1	76.3 (4.4); 65.9 - 84	78.5 (9.3); 63.4 - 96.8	87.5 (5.2); 78.4 - 94.3
2013	78.2 (1.4); 76.2 - 79.6	77 (7); 67 - 89.3	80.2 (8.2); 53.4 - 95.3	82.9 (6.1); 71 - 94.7
2014	92.9 (6.3); 83.7 - 97.9	79.8 (5.5); 71.7 - 92.1	80.4 (7.3); 64.6 - 98.8	89.4 (3.9); 83.6 - 95.5

Discussion

The *Pd* screening investigation did not result in the detection of the pathogen. However, the culturing methodology resulted in the detection of sequences associated with *Geomyces* (GenBank ID: JX270486.1, JX270246.1) and *Pseudogymnoascus* (GenBank IDs: KP902680.1, LN852362.1) in Egypt Cave sample EGGU08. These sequences likely represent undescribed taxa within the respective genus (Lorch et al. 2012). While neither of the detected *Geomyces* or

Pseudogymnoascus sequences are associated with *Pd*, these highlight the importance of monitoring caves in central Texas for the pathogen, as members of these genera are commonly isolated from soil in cool environments (Domsch et al. 2007 in Lorch et al. 2012). The detections of these closely related taxa, in addition to the recorded microclimate data, indicate that the study caves, especially Shell Mountain and Egypt, offer potential refuge for the causative agent of WNS. As a psychrophilic fungus, *Pd* is known to thrive in temperatures between 7 and 16°C (Langwig et al. 2012; Verant et al. 2012; Langwig et al. 2014), with upper critical temperature limits extending to nearly 20°C (Verant et al. 2012).

With potentially suitable habitat present in central Texas caves and known migratory pathways for bats extending to northern Texas, it is possible that a detection of *Pd* could occur in the region within the near future. While unsurprising, the negative findings of this screening study will contribute to a better understanding of the spread of WNS by filling regional data gaps. In addition, gaining a better understanding of the ecology of cave microflora may be key to understanding and managing the progression of WNS in hibernating bats, and an expansion of the analysis of the fungal communities in the study caves at Fort Hood would continue to fill data gaps for the epidemiological understanding of the disease and mycological studies in cave environments. Opportunities for research expansion include developing species richness and diversity records for the study caves to monitor changes in the fungal community over time and incorporating additional study sites used by bats such as rock shelters and access tunnels on the Fort Hood installation. Despite the anticipated negative screening results based on the current, known locations of the pathogen in North America, regular surveillance of *Pd* at Fort Hood and other DoD installations with bats inhabiting cave roosts, particularly those harboring protected species, will assist DoD land managers in contributing to mission readiness by demonstrating proactive resource management in the event of positive detection.

Several of the genera identified in this study are some of the most commonly reported taxa from cave mycology studies, including *Aspergillus*, *Penicillium*, *Mucor*, *Fusarium*, *Alternaria*, *Chrysosporium*, and *Chaetomium* (Vanderwolf et al. 2013). Unsurprisingly, many of these taxa are ubiquitous, commonly occurring as saprobes in the soil, air, or in plant litter or other detritus, and often function as facultative pathogens of humans, other animals, and plants. Species of *Aspergillus* are often are treated as allergens in humans, especially associated with water-damaged buildings, and both *A. fumigatus* and *A. sclerotiorum* have been noted as human pathogens (Pfaller and Diekema 2004; Negroni 2010). *Fusarium* species are known to produce numerous mycotoxins and cause a wide range of infections in humans, animals, and plants (Desjardins and Proctor 2007). Although not commonly reported from caves, other species that are pathogenic or allergenic to humans were isolated, including *Curvularia* (Nieves-Rivera 2003; KoilRaj et al. 2012; Karkun et al. 2012; Taylor et al. 2013) and *Trichosporon* (Sugita et al. 2005; Nováková, et al. 2009).

The apparent detection of the two *Phialosimplex* species in Egypt Cave is intriguing. This anamorphic genus within the Trichocomaceae family of Ascomycota was only recently described (Sigler et al. 2010), and there are relatively few reports from the environment (i.e., non-clinical)

in recent literature. Species of this genus, including *P. chlamydosporus*, are known to be associated with infections in canines (Sigler et al. 2010), and at least one of its members is known to be halotolerant, as several strains of *P. salinarum* were isolated from subterranean waters in a salt mine in Germany (Greiner et al. 2014). While the identity match scores for these two species were somewhat low (91 to 93%), the results include a reasonable length of matching nucleotides for identification for both sequences (480 to 559 nt). These sequence results could indicate the presence of an undescribed species within the genus *Phialosimplex*. Given the relative lack of information on this genus and the occurrence of its members in cave habitats, additional investigations into the phylogeny of these recovered sequences are warranted.

Literature Cited

AGFC. 2015b. White-nose syndrome found in more Ouachita, Ozarks bats. May 27, 2015 Arksansas Outdoors Weekly Newsleter. Retrieved 30 July 2015 from http://www.agfc.com/Pages/newsDetails.aspx?show=946.

Arkansas Game and Fish Commission (AGFC). 2015a. White-nose syndrome found in bats in Independence, Newton, and Madison counties. Retrieved 30 July 2015 from http://www.agfc.com/Pages/newsDetails.aspx?show=912.

Blehert D.S., A.C. Hicks, M. Behr, C.U. Meteyer, B.M. Berlowski-Zier, E.L. Buckles, J.T. Coleman, S.R. Darling, A. Gargas, R. Niver, J.C. Okoniewski, R.J. Rudd, and W.B. Stone. 2009. Bat white-nose syndrome: an emerging fungal pathogen? Science, 323(5911):227.

Boyle, D.G., D.B. Boyle, V. Olsen, J.A.T. Morgan, and A.D. Hyatt. 2004. Rapid quantitative detection of chytridiomycosis (*Batrachochytrium dendrobatidis*) in amphibian samples using real-time Taqman PCR assay. Diseases of aquatic organisms, 60, 141-148.

Canadian Wildlife Health Cooperative. 2015. A national plan to manage White Nose Syndrome in bats in Canada. Western College of Veterinary Medicine, University of Saskatchewan. Saskatoon, Saskatchewan, Canada. http://www.cwhc-rcsf.ca/docs/BatWhiteNoseSyndrome-NationalPlan.pdf

Chillali M., H. Idder-Ighili, and J.J. Guillaumin. 1998. Variation in the ITS and IGS regions of ribosomal DNA among the biological species of European Armillaria. Mycological Research, 102: 533–540.

Colombo, A.L., A.C.B. Padovan, and G.M. Chaves. 2011. Current knowledge of Trichosporon spp. and trichosporonosis. *Clinical microbiology reviews*, *24*(4), 682-700.

Cryan, P. M., C.U. Meteyer, J.G. Boyles, and D.D. Blehert. 2010. Wing pathology of white-nose syndrome in bats suggests life-threatening disruption of physiology. BMC biology. 8(1), 135.

Cryan, P. M., C.U. Meteyer, D.S. Blehert, J.M. Lorch, D.M. Reeder, G.G. Turner, J. Webb, M. Behr, M. Verant, R.E. Russel, and K.T. Castle. 2013. Electrolyte depletion in white-nose syndrome bats. Journal of Wildlife Diseases, 49(2), 398-402.

Desjardins, A.E. and R.H. Proctor. 2007. Molecular biology of *Fusarium* mycotoxins. *International journal of food microbiology*, *119*(1), 47-50.

Domsch, K.H., W. Gams, and T.H. Anderson. 1980. Compendium of soil fungi. Volume 1, Number 2. London: Academic press.

Feliner, G. N. and J.A. Rosselló. 2007. Better the devil you know? Guidelines for insightful utilization of nrDNA ITS in species-level evolutionary studies in plants. *Molecular phylogenetics and evolution*, *44*(2), 911-919.

Gargas A., M.T. Trest, M. Christiensen, T.J. Volk, D.S. Blehert. 2009. *Geomyces destructans* sp. nov. associated with bat white-nose syndrome. Mycotaxon, 108:147–54.

Hajibabaei, M., M. Smith, D.H. Janzen, J.J. Rodriguez, J.B. Whitfield, and P.D. Hebert. 2006. A minimalist barcode can identify a specimen whose DNA is degraded. Molecular Ecology Notes, 6(4), 959-964.

Hillis, D. M. and M.T. Dixon. 1991. Ribosomal DNA: molecular evolution and phylogenetic inference. *Quarterly Review of Biology*, 411-453.

Jackson, C. J., R.C. Barton, and E.G.V. Evans. 1999. Species identification and strain differentiation of dermatophyte fungi by analysis of ribosomal-DNA intergenic spacer regions. *Journal of clinical microbiology*, *37*(4), 931-936.

Karkun, A., K.L. Tiwari, and S.K. Jadhav. 2012. Fungal diversity of Mandeepkhol Cave in Chhattisgarh, India. *Advances in Bioresearch*, *3*(2), 119-123.

KoilRaj, A.J., P. Prabhavathi, R. Rajendran, T. Kuberan, R.S. Gowri, and C.P. Selvi. 2012. Degradation of organic wastes and recycling of nutrients enhanced by microbes in subterranean habitat. *African Journal of Microbiology Research*, *6*(21), 4449-4456.

Kõljalg U., R.H. Nilsson, K. Abarenkov, L. Tedersoo, A.F.S. Taylor, M. Bahram, S.T. Bates, T.D. Bruns, J. Bengtsson-Palme, T.M. Callaghan et al. 2013. Towards a unified paradigm for sequence-based identification of fungi. *Molecular Ecology* **22**: 5271–5277.

Krizsán, K., T. Papp, P. Manikandan, C.S. Shobana, M. Chandrasekaran, C. Vágvölgyi, and L. Kredics. 2015. Clinical importance of the cenus *Curvularia*. *Medical Mycology: Current Trends and Future Prospects*, 147.

Langwig, K.E., W.F. Frick, J.T. Bried, A.C. Hicks, T.H. Kunz, and A. Marm Kilpatrick. 2012. Sociality, density-dependence and microclimates determine the persistence of populations suffering from a novel fungal disease, white-nose syndrome. Ecology Letters, 15(9), 1050-1057.

Langwig, K.E., W.F. Frick, R. Reynolds, K.L. Parise, K.P. Drees, J.R. Hoyt, T.L. Cheng, T.H. Kunz, J.T. Foster, and A.M. Kilpatrick. 2015. Host and pathogen ecology drive the seasonal dynamics of a fungal disease, white-nose syndrome. *Proceedings of the Royal Society of London B: Biological Sciences*, *282*(1799), 20142335.

Lorch, J.M., C.U. Meteyer, M.J. Behr, J.G. Boyles, P.M. Cryan, A.C. Hicks, A.E. Ballmann, J.T.H. Coleman, D.N. Redell, D.M. Reeder, and D.S. Blehert. 2011. Experimental infection of bats with *Geomyces destructans* causes white-nose syndrome. Nature. 480:376-378.

Lorch, J.M., D.L. Lindner, A. Gargas, L.K. Muller, A.M. Minnis, and D.S. Blehert. 2012. A culture-based survey of fungi in soil from bat hibernacula in the eastern United States and its implications for detection of *Geomyces destructans*, the causal agent of bat white-nose syndrome. Mycologia, 12-207.

Martínková, N., P. Bačkor, T. Bartonička, P. Blažková, J. Červený, L. Falteisek, J. Gaisler, V. Hanzal, D. Horáček, Z. Hubálek, H. Jahelková, M. Kolaøík, L. Korytár, A. Kubátová, B. Lehotská, R. Lehotský, R.K. Lučan, O. Májek, J. Matějù, Z. Rehák, J. Šafář, P. Tájek, E. Tkadlec, M. Uhrin, J. Wagner, D. Weinfurtová, J. Zima, J. Zukal, and I. Horáček. 2010. Increasing incidence of *Geomyces destructans* fungus in bats from the Czech Republic and Slovakia. PLoS One, 5(11), e13853.

Meteyer C.U., E.L. Buckles, D.S. Blehert, A.C. Hicks, D.E. Green, V. Shearn-Bochsler, N.J. Thomas, A. Gargas, and M.J. Behr. 2009. Histopathologic criteria to confirm white-nose syndrome in bats. Journal of Veterinary Diagnostic Investigation, 21(4), 411-414.

Middlehoven, W.J. 2003 Identification of clinically relevant *Trichosporon* species. Mycoses 46:7–11.

Middlehoven, W.J. 2004. *Trichosporon wieringae* sp. nov., an anamorphic basidiomycetous yeast from soil, and assimilation of some phenolic compounds, polysaccharides and other non-conventional carbon sources by saprophytic *Trichosporon* species. Antonie Van Leeuwenhoek 86:329–337.

Min, X.J. and D.A. Hickey. 2007. Assessing the effect of varying sequence length on DNA barcoding of fungi. Molecular Ecology Notes, 7(3), 365-373.

Minnis, A. M. and D.L. Lindner. 2013. Phylogenetic evaluation of *Geomyces* and allies reveals no close relatives of *Pseudogymnoascus destructans*, comb. nov., in bat hibernacula of eastern North America. Fungal biology, 117(9), 638-649.

Muller, L. K., J.M. Lorch, D.L. Lindner, M. O'Connor, A. Gargas, and D.S. Blehert. 2013. Bat white-nose syndrome: a real-time TaqMan polymerase chain reaction test targeting the intergenic spacer region of Geomyces destructans. *Mycologia*, *105*(2), 253-259.

Negroni, R. 2010. Onychomycosis Due to Aspergillus Species. In *Aspergillosis: From Diagnosis to Prevention* (pp. 961-971). Springer Netherlands.

Nieves-Rivera, Á.M. 2003. Mycological survey of Río Camuy Caves Park, Puerto Rico. *Journal of Cave and Karst Studies*, *65*(1), 23-28.

Nováková, A. 2009. Microscopic fungi isolated from the Domica Cave system (Slovak Karst National Park, Slovakia). A review. *International Journal of Speleology*, *38*(1), 8.

Oklahoma Department of Wildlife Conservation. 2015. Fungus responsible for bat disease found in state. Retrieved 30 July 2015 from http://wildlifedepartment.com/media/bfungus.htm.

Pekins, C. E. 2012. Cave Myotis (*Myotis velifer incautus*) Population and roost microclimate monitoring at a maternity site on Fort Hood, Texas during 2011-2012. Unpublished report for DPW-ENV-Natural Resources Branch, Fort Hood, Texas, USA.

Pfaller, M.A. and D.J. Diekema. 2004. Rare and emerging opportunistic fungal pathogens: concern for resistance beyond *Candida albicans* and *Aspergillus fumigatus*. *Journal of Clinical Microbiology*, *42*(10), 4419-4431.

Puechmaille, S. J., P. Verdeyroux, H. Fuller, M.A. Gouilh, M. Bekaert, and E.C. Teeling. 2010. White-nose syndrome fungus (*Geomyces destructans*) in bat, France. Emerging infectious diseases, 16(2), 290.

Puechmaille S.J., G. Wibbelt, V. Korn, H. Fuller, F. Forget, K. Mühldorfer, et al. 2011. Pan-European distribution of white-nose syndrome fungus (*Geomyces destructans*) not associated with mass mortality. PLoS ONE 6(4): e19167.

Reddell, J. R., J. Fant, C. Pekins, M. Reyes, and M. Warton. 2015. Karst research on Fort Hood, Bell and Coryell Counties, Texas. Unpublished report prepared for U.S. Army Garrison, DPW-Environmental Division, Natural Resources Management Branch, Fort Hood, Texas, USA. 1032 pp.

Reeder, D. M., C.L. Frank, G.G. Turner, C.U. Meteyer, A. Kurta, E.R. Britzke, M.E. Vodzak, S.R. Darling, C.W. Stihler, A.C. Hicks, R. Jacob, L.E. Grieneisen, S.A. Brownlee, L.K. Muller, and D.S. Blehert. 2012. Frequent arousal from hibernation linked to severity of infection and mortality in bats with white-nose syndrome. PLoS One, 7(6), e38920.

Reichard J.D. and T.H. Kunz. 2009. White-nose syndrome inflicts lasting injuries to the wings of little brown myotis (*Myotis lucifugus*). Acta Chiropterologica, 11(2):457–64

Schoch C.L., K.A. Seifert, S. Huhndorf, V. Robert, J.L. Spouge, C.A. Levesque, and W. Chen. 2012. Nuclear ribosomal internal transcribed spacer (ITS) region as a universal DNA barcode marker for Fungi. Proceedings of the National Academy of Sciences, USA 109: 6241–6246.

Sigler, L., D.A. Sutton, C.F.C. Gibas, R.C. Summerbell, R.K. Noel, and P.C. Iwen. 2010. *Phialosimplex*, a new anamorphic genus associated with infections in dogs and having phylogenetic affinity to the Trichocomaceae. *Medical Mycology*, *48*(2), 335-345.

Skouboe P., J.C. Frisvad, and J.W. Taylor. 1999. Phylogenetic analysis of nucleotide sequences from the ITS region of terverticillate *Penicillium* species. Mycological Research, 103: 873–881.

Sugita T., A. Nishikawa, T. Ichikawa, R. Ikeda, and T. Shinoda. 2000. Isolation of *Trichosporon asahii* from environmental materials. Medical Mycology 38:27–30.

Sugita, T., M. Nakajima, R. Ikeda, T. Matsushima, and T. Shinoda. 2002. Sequence analysis of the ribosomal DNA intergenic spacer 1 regions of *Trichosporon* species. Journal of Clinical Microbiology. 40:1826–1830.

Sugita, T., K. Kikuchi, K. Makimura, K. Urata, T.Someya, K. Kamei, M. Niimi, and Y. Uehara. 2005. *Trichosporon* species isolated from guano samples obtained from bat-inhabited caves in Japan. Applied and environmental microbiology,71(11), 7626-7629.

Suh, S.O. and M. Blackwell. 2004. Three new beetle-associated yeast species in the *Pichia guilliermondii* clade. FEMS Yeast Research, 4:87–95.

Suh S.O., J.V. McHugh, D.D. Pollock, and M. Blackwell. 2005. The beetle gut: a hyperdiverse source of novel yeasts. Mycological Research, 109:261–265.

Taylor, E.L.S., M.A.D. Resende Stoianoff, and R. Lopes Ferreira. 2013. Mycological study for a management plan of a neotropical show cave (Brazil).International Journal of Speleology, 42(3), 10.

U.S. Geological Survey (USGS) – National Wildlife Health Center (NWHC). Appendix E – Protocol for non-lethal swab sampling of bat skin for detection of *Pseudogymnoascus destructans* (*Pd*). Revised 6/11/2014

USGS NWHC. 2010. *Geomyces destructans* detected in Oklahoma cave myotis and listed Missouri gray bats. Wildlife Health Bulletin #2010-04. Retrieved 24 June 2015 from http://www.nwhc.usgs.gov/publications/wildlife_health_bulletins/WHB_10_04.jsp.

USGS NWHC. 2014. White-nose syndrome updates for the 2013/2014 surveillance season. Wildlife Health Bulletin #2014-04. Retrieved 24 June 2015 from http://www.nwhc.usgs.gov/publications/wildlife_health_bulletins/WHB_2014-04_WNS_Updates.pdf.

U.S. Fish and Wildlife Service (USFWS). 1994. 50 CFR part 17. Endangered and threatened wildlife and plants: Animal candidate review for listing as endangered or threatened species: Federal Register 59: 58982-59028.

USFWS. 2011. A national plan for assisting states, federal agencies, and tribes in managing white-nose syndrome in bats. May 2011.

USFWS. 2015a. Bats affected by WNS. Retrieved 30 July 2015 from https://www.whitenosesyndrome.org/about/bats-affected-wns.

USFWS. 2015b. White-nose syndrome map. Retrieved 29 July 2015 from https://www.whitenosesyndrome.org/resources/map.

Vanderwolf, K.J., D. Malloch, D.F. McAlpine, and G.J. Forbes. 2013. A world review of fungi, yeasts, and slime molds in caves. *International Journal of Speleology*, *42*(1), 9.

Verant, M. L., M.U. Carol, J.R. Speakman, P.M. Cryan, J.M. Lorch, and D.S. Blehert. 2014. White-nose syndrome initiates a cascade of physiologic disturbances in the hibernating bat host. BMC physiology. 14(1), 10.

Vialle A., N. Feau, M. Allaire, M. Didukh, F. Martin, J. Moncalvos, and R. Hamelin. 2009. Evaluation of mitochondrial genes as DNA barcode for Basidiomycota. Molecular Ecology Resources, 9: 99-113.

Warnecke, L., J.M. Turner, T.K. Bollinger, J.M. Lorch, V. Misra, P.M. Cryan, G. Wibbelt, D.M. Blehert, and C.K. Willis. 2012. Inoculation of bats with European *Geomyces destructans* supports the novel pathogen hypothesis for the origin of white-nose syndrome. Proceedings of the National Academy of Sciences, 109(18), 6999-7003.

Warnecke, L., J.M. Turner, T.K. Bollinger, V. Misra, P.M. Cryan, D.S. Blehert, G. Wibbelt, and C.K. Willis. 2013. Pathophysiology of white-nose syndrome in bats: a mechanistic model linking wing damage to mortality. Biology letters, 9(4), 20130177.

Wibbelt, G., A. Kurth, D. Hellmann, M. Weishaar, A. Barlow, M. Veith, J. Prüger, T. Görföl, L. Grosche, F. Bontadina, U. Zöphel, H.P. Seidl, P.M. Cryan, and D.S. Blehert. 2010. White-nose syndrome fungus (*Geomyces destructans*) in bats, Europe. Emerging infectious diseases, 16(8), 1237.

White, T. J., T. Bruns, S. Lee, and J. W. Taylor. 1990. Amplification and direct sequencing of fungal ribosomal RNA genes for phylogenetics. Pp. 315-322 In: PCR Protocols: A Guide to Methods and Applications, eds. Innis, M. A., D. H. Gelfand, J. J. Sninsky, and T. J. White. Academic Press, Inc., New York.